Journal of Sound and Vibration (2002) **251**(4), 579–619
doi:10.1006/jsvi.2001.3713, available online at http://www.idealibrary.com on IDEAL®

GEOMETRICALLY NON-LINEAR FREE VIBRATION OF FULLY CLAMPED SYMMETRICALLY LAMINATED RECTANGULAR COMPOSITE PLATES

B. HARRAS AND R. BENAMAR

Laboratoire d'Etudes et de Recherches en Simulation, Instrumentation et Mesure, LERSIM, E. G. T., Ecole Mohammadia d'Ingénieurs, Université Mohammed V, BP 765 Agdal, Robat, Morocco.
E-mail: rbenamar@emi.ac.ma

AND

R. G. WHITE

*Department of Aeronautics and Astronautics, University of Southampton S*017 1*BJ, England*

(*Received* 9 *August* 2000, *and in final form* 20 *February* 2001)

The geometrically non-linear free vibration of thin composite laminated plates is investigated by using a theoretical model based on Hamilton's principle and spectral analysis previously applied to obtain the non-linear mode shapes and resonance frequencies of thin straight structures, such as beams, plates and shells (Benamar *et al.* 1991 *Journal of Sound and Vibration* **149**, 179–195; 1993, **164**, 295–316; 1990 *Proceedings of the Fourth International Conference on Recent Advances in Structural Dynamics, Southampton*; *Moussaoui et al.* 2000 *Journal of Sound and Vibration* **232**, 917–943 [1–4]). The von Kármán non-linear strain–displacement relationships have been employed. In the formulation, the transverse displacement W of the plate mid-plane has been taken into account and the in-plane displacements U and V have been neglected in the non-linear strain energy expressions. This assumption, quite often made in the literature has been adopted in reference [2] and (El Kadiri *et al.* 1999 *Journal of Sound and Vibration* **228**, 333–358 [5]), in the isotropic case and has been mentioned here because the results obtained have been found to be in very good agreement with those based on the hierarchical finite element method (HFEM). In a previous study, it was assumed, based on the analogy with the isotropic case, that the fundamental carbon fibre reinforced plastic (CFRP) plate non-linear mode shape could be well estimated, by using nine plate functions, obtained as products of clamped–clamped beam functions in the x and y directions, symmetric in both the length and width directions [3]. In the present work, a convergence study has been performed and has shown that, although such an assumption may yield a good estimate for the non-linear resonance frequency, 18 plate functions should be taken into account instead of nine in the first non-linear mode shape and associated bending stress patterns calculations. This allows the anisotropy induced by the fibre orientations to be taken into account. Results are given for the fundamental mode of fully clamped CFRP rectangular plates, for various plate aspect ratios and vibration amplitudes. The non-linear mode shows a higher bending stress near the clamps at large deflection, compared with that predicted by linear theory. Some experimental measurements are presented which are in good qualitative agreement with the theory.

1. INTRODUCTION

There is a continually increasing interest in the use of composite materials in many industrial fields. This is due to their now well-known properties, which allow efficient use of

0022-460X/02/140579 + 41 $35.00/0

the material through appropriate tailoring and suitable choice of fibre orientation. Indeed, composite materials present considerable potential for wide use in aircraft structures in the future [6–9], especially because of their advantages of improved toughness, reduction in structural weight, reduction in fatigue and corrosion problems, the two latter considerations being of vital significance. These are the reasons why CFRP materials have been used as structural members, taking the place of traditional metals [7]. Aluminium alloy is generally used in commercial aircraft and composite laminated constructions are more widely used in military aircraft, particularly in smaller-sized aircraft [10].

The use of composite materials requires complex analytical methods in order to predict accurately their response to external loading, especially in severe environments, which may induce geometrically non-linear behaviour [11]. This requires appropriate design criteria and accurate estimation of the fatigue life [11–14]. In addition to the usual difficulties encountered generally in the non-linear analysis of structures, related to the fact that the theorem of superposition does not hold, existence and uniqueness of the solutions are generally not guaranteed [15]. The geometrically non-linear analysis of composite plates exhibits specific difficulties due to the anisotropic material behaviour, and to the higher non-linearity induced by a higher stiffness, inducing tensile mid-plane forces in plates higher, than that observed with conventional homogeneous materials [11, 16, 17].

Without attempting a comprehensive review, some important works and methodological approaches to the problem of non-linear dynamic response of plates at large vibration amplitudes will be mentioned here in order to introduce the subject and locate the present work with respect to the current state of knowledge.

The study of the non-linear free and forced dynamic responses at large vibration amplitudes of homogeneous and composite plates of various geometries has been a subject of numerous experimental and theoretical investigations during the last few decades. In the excellent monograph of Leissa [18], complemented by the journal paper [19], a summary of the knowledge and information on linear dynamic isotropic plate problems has been presented. Some references have also been given which are concerned with the large vibration amplitude problem, and have been considered as a good introduction to geometric type one-linearity [20]. Whitney and Leissa [21] have formulated the governing equations for non-linear vibrations of anisotropic plates based on the von Kármán theory. In the series of studies carried out by White and his co-workers [11–13, 16, 17, 22–26], a wide programme of experimental work was concentrated on the understanding of the dynamic behaviour of homogeneous and CFRP beams and plates. Chia, in his book [27], gave extensive information on the non-linear analysis of plates, with presentation of a variety of geometrically non-linear static and dynamic problems. In reference [28], a survey was presented of the literature on the geometric non-linear analysis of laminated composite elastic plates. Sathyamoorthy [20] has presented a review which deals with analytical, numerical and experimental methods used in the geometrically non-linear dynamic analysis of plates. A comprehensive survey of the finite element method applied to non-linear vibration has been also presented. A recent review of current developments in non-linear vibration analysis has been presented in reference [29], which includes different methods of analysis and references to experimental studies [11–13, 17, 22–26].

The classical finite element method (FEM) can also be used for accurate solution of complex engineering problems. One of the first works in which the FEM was applied to the geometrically non-linear dynamics of structures was that of Mei [30–32] followed by others [33, 34]. Recent investigations carried out by Petyt and his co-workers [35–40] have been presented dealing with the geometrically non-linear dynamic behaviour of symmetrically laminated plates by using the hierarchical finite element method (HFEM). In reference [40], the HFEM and Harmonic Balance Method have been used to analyze the free vibration

with large displacements of thin, rectangular, composite symmetrically laminated, fully clamped plates. The convergence with the number of harmonics and with the number of shape functions has been discussed. Internal resonances have been detected and their effect on the dynamic behaviour of the laminated plates considered has been described. An asymptotic-numerical method based on a combination of a perturbation technique and the FEM has been developed in reference [41] for studying the large amplitude free vibrations of thin elastic plates. In spite of a considerable amount of research and a wide variety of methodological approaches, the finite element method (FEM) remains the only way for dealing with complex structures, and the most versatile. However, in the FEM formulation of non-linear vibration problems, the solution of the non-linear equations of motion can be obtained only approximately and iteratively [40]. Also, the formulation is quite laborious and the time needed to obtain the solutions increases considerably with the number of degrees of freedom (d.o.f.) [40].

In a series of papers by Benamar and co-workers [1–5, 17, 42–46], a theoretical model based on Hamilton's principle and spectral analysis has been developed to study the non-linear free and steady state periodic forced vibrations of beams, and the non-linear free vibration of homogeneous and composite plates and shells. This model is based on analytical and numerical procedures and the assumptions are the separation of the time and space variables and harmonic dependence in time. In reference [1], the first three non-linear mode shapes of clamped–clamped and simply supported beams have been obtained by using the above model. The results obtained corresponding to the fundamental non-linear mode shape were in good agreement with those of a previous theoretical and experimental study [47]. In reference [2], the theoretical model, established and applied to beams in reference [1], was extended to the fully clamped rectangular plate case. The first non-linear mode shape has been investigated both theoretically and experimentally. Experimental measurements were in good agreement with the theory. El Kadiri *et al.* [5] used this model to calculate the second non-linear mode shape of fully clamped rectangular homogeneous plate for various values of the aspect ratio, and analyzed the effect of non-linearity on the induced bending stresses. Good agreement was obtained in comparison with other results. Azrar *et al.* [44] adapted the model presented in references [1–3] to study the non-linear steady state forced response of C–C and S–S beams; the results obtained were close to those obtained by other methods. Recently, this method has been extended to the non-linear free vibration of cylindrical shells by Moussaoui *et al.* [4]. The effects of large vibration amplitudes on the first and second coupled transverse-circumferential mode shapes of isotropic circular cylindrical shells of infinite length have been examined. More recently, this method has been extended to the non-linear free vibration of clamped circular plates and C–C–C–SS plates [45, 46]. Good agreement has been found in each case with previous published works.

The aim of this paper is to apply the theoretical model developed in references [1–3] to analyze the geometrical non-linear free dynamic response of rectangular CFRP symmetrically laminated plates in order to investigate the effect of non-linearity on the non-linear resonance frequencies and the non-linear fundamental mode shape and associated bending stress patterns at large vibration amplitudes. The general formulation of the model for non-linear vibration of laminated plates at large vibration amplitudes is presented. Periodic displacement was assumed since the motion of plates vibrating freely with amplitude displacements of the order of their thickness is generally periodic [48]. Fully clamped boundaries have been considered here because they are adequate to model many real panel-type situations, such as aircraft wing panels [49] and are the easiest to achieve in practice, compared with the simply supported boundaries, for experimental measurements. The first non-linear mode shape is examined. The relationships between the non-linear

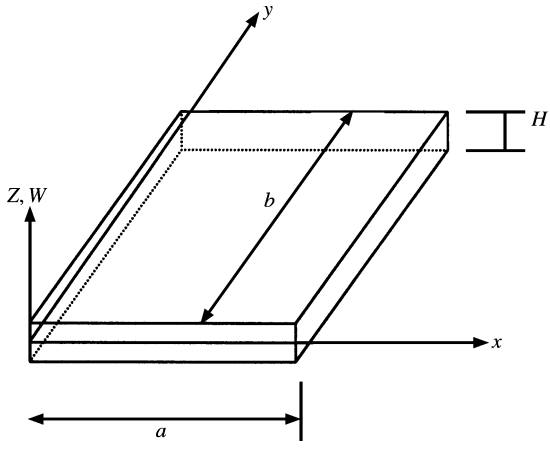

Figure 1. Plate notation.

resonance frequency ratio ω_{nl}/ω_l and the vibration amplitudes, and between the maximum vibration amplitude and the first non-linear mode shape, for various plate aspect ratios are discussed. Comparison of the change in natural frequency at large vibration amplitudes, and in bending stress patterns, between isotropic and CFRP plates is presented. Some experimental measurements for the first non-linear mode shape are also reported and discussed. The second non-linear mode shape and the analysis of the fibre orientation effect will be presented later.

2. FORMULATION OF THE GEOMETRICALLY NON-LINEAR FREE VIBRATION OF FULLY CLAMPED SYMMETRICALLY LAMINATED RECTANGULAR COMPOSITE PLATES

2.1. CONSTITUTIVE EQUATION OF A LAMINATED PLATE AT LARGE DEFLECTIONS

Consider the transverse vibration of the plate shown in Figure 1 of dimensions a, b and H with a co-ordinate system taken such that the xy plane coincides with the mid-plane of the plate.

For the classical plate laminated theory [50], the strain–displacement relationship for large deflections are given by [51]

$$\{\varepsilon\} = \{\varepsilon^0\} + z\{\kappa\} + \{\lambda^0\}, \tag{1}$$

in which $\{\varepsilon^0\}$, $\{\kappa\}$ and $\{\lambda^0\}$ are given by

$$\{\varepsilon^0\} = \begin{bmatrix} \varepsilon_x^0 \\ \varepsilon_y^0 \\ \gamma_{xy}^0 \end{bmatrix} = \begin{bmatrix} \dfrac{\partial U}{\partial x} \\ \dfrac{\partial V}{\partial y} \\ \dfrac{\partial U}{\partial y} + \dfrac{\partial V}{\partial x} \end{bmatrix}, \qquad \{\kappa\} = \begin{bmatrix} \kappa_x \\ \kappa_y \\ \kappa_{xy} \end{bmatrix} = \begin{bmatrix} -\dfrac{\partial^2 W}{\partial x^2} \\ -\dfrac{\partial^2 W}{\partial y^2} \\ -2\dfrac{\partial^2 W}{\partial xy} \end{bmatrix} \tag{2, 3}$$

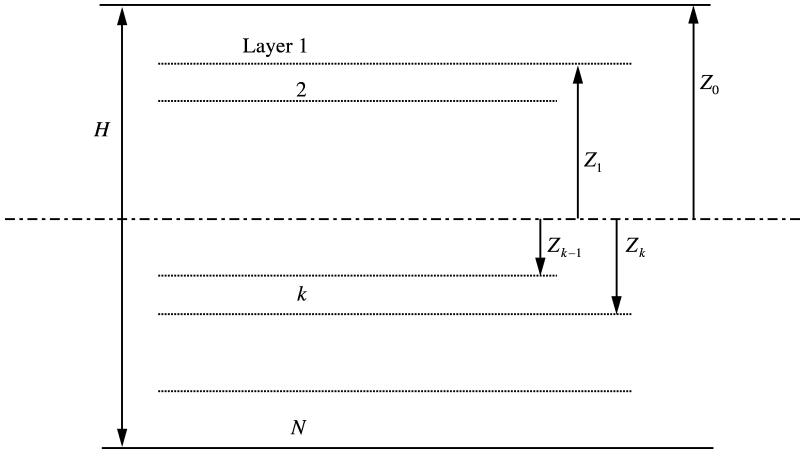

Figure 2. Geometry of n layered laminated plate.

$$\{\lambda^0\} = \begin{bmatrix} \lambda_x^0 \\ \lambda_y^0 \\ \lambda_{xy}^0 \end{bmatrix} = \begin{bmatrix} \frac{1}{2}\left(\frac{\partial W}{\partial x}\right)^2 \\ \frac{1}{2}\left(\frac{\partial W}{\partial y}\right)^2 \\ \frac{\partial W}{\partial x}\frac{\partial W}{\partial y} \end{bmatrix}. \tag{4}$$

U, V and W are displacements of the plate mid-plane, in the x, y and z directions respectively. (A list of nomenclature is given in Appendix B.)

For the laminated plate having n layers as shown in Figure 2, the stress in the kth layer can be expressed in terms of the laminated middle surface strains and curvatures as

$$\{\sigma_k\} = [\bar{Q}]_k\{\varepsilon\}, \tag{5}$$

in which $\{\sigma\}_k^{\mathrm{T}} = [\sigma_x\ \sigma_y\ \tau_{xy}]$ and terms of the matrix $[\bar{Q}]$ can be obtained by the relationships given in reference [52].

The force and moment resultants for the kth layer are defined as

$$(N_x^{(k)}, N_y^{(k)}, N_{xy}^{(k)}) = \int_{h_{k-1}}^{h_k} (\sigma_x^{(k)}, \sigma_y^{(k)}, \sigma_{xy}^{(k)})\,\mathrm{d}z, \tag{6}$$

$$(M_x^{(k)}, M_y^{(k)}, M_{xy}^{(k)}) = \int_{h_{k-1}}^{h_k} (\sigma_x^{(k)}, \sigma_y^{(k)}, \sigma_{xy}^{(k)})z\,\mathrm{d}z, \tag{7}$$

where h_k is the distance from the mid-plane to the surface of the kth layer.

The in-plane forces and bending moments in a plate are given by

$$\begin{bmatrix} N \\ M \end{bmatrix} = \begin{bmatrix} A & B \\ B & D \end{bmatrix} \begin{bmatrix} \{\varepsilon^0\} + \{\lambda^0\} \\ \{\kappa\} \end{bmatrix}. \tag{8}$$

A, B and D are the symmetric matrices given by the following equation (9). $[B] = 0$ for symmetrically laminated plates [53]:

$$(A_{ij}, B_{ij}, D_{ij}) = \int_{-H/2}^{H/2} Q_{ij}^{(k)}(1, z, z^2)\,\mathrm{d}z. \tag{9}$$

Here the $Q_{ij}^{(k)}$ are the reduced stiffness coefficients of the kth layer in the plate co-ordinates.

The expression for the bending strain energy V_b, axial strain energy V_a and kinetic energy T are given by [50]

$$V_b = \frac{1}{2}\int_S \left\{ D_{11}\left(\frac{\partial^2 W}{\partial x^2}\right)^2 + 2D_{12}\frac{\partial^2 W}{\partial y^2}\frac{\partial^2 W}{\partial x^2} + D_{22}\left(\frac{\partial^2 W}{\partial y^2}\right)^2 + 4D_{16}\frac{\partial^2 W}{\partial x^2}\frac{\partial^2 W}{\partial xy} + 4D_{26}\frac{\partial^2 W}{\partial y^2}\frac{\partial^2 W}{\partial xy} + 4D_{66}\left(\frac{\partial^2 W}{\partial xy}\right)^2 \right\}\mathrm{d}S, \tag{10}$$

$$V_a = \frac{1}{2}\int_S \left\{ \frac{A_{11}}{4}\left(\frac{\partial W}{\partial x}\right)^4 + \frac{A_{22}}{4}\left(\frac{\partial W}{\partial y}\right)^4 + \left[\frac{A_{12}}{2} + A_{66}\right]\left(\frac{\partial W}{\partial y}\right)^2\left(\frac{\partial W}{\partial x}\right)^2 + A_{16}\left(\frac{\partial W}{\partial x}\right)^3\frac{\partial W}{\partial y} + A_{26}\left(\frac{\partial W}{\partial y}\right)^3\frac{\partial W}{\partial x} \right\}\mathrm{d}S \tag{11}$$

and

$$T = \frac{1}{2}\rho H \int_S \left(\frac{\partial W}{\partial t}\right)^2 \mathrm{d}S, \tag{12}$$

where S is the plate surface $[0, a] \times [0, b]$ and $\mathrm{d}S$ is the elementary surface $\mathrm{d}x\ \mathrm{d}y$.

In the above expressions, the assumption of neglecting the in-plane displacements U and V in the energy expressions has been made as for the fully clamped rectangular isotropic plates analysis considered in references [2, 5]. The range of validity of this assumption has been extensively discussed in the light of the experimental and numerical results obtained for the frequency amplitude dependence and the bending stress estimates obtained at large vibration amplitudes. The results obtained via this assumption were compared with the previous ones based on various methods such as the finite element method, the method based on Berger's approximation, the ultraspherical polynomial method and the elliptic function method. It was found that the percentage error in the non-linear frequency estimates based on this assumption, for amplitudes up to 1·5 times thickness, does not exceed 1·3%. Also, in the experimental investigation of the non-linear behaviour of fully clamped rectangular plates at large vibration amplitudes presented in reference [43], it was found that the rate of increase in bending stresses estimates, obtained from measured data, was in very good agreement with that obtained from the theory, in which the assumption of zero in-plane displacements was made. The above references were concerned with the isotropic case. It has led to the conclusion that this assumption allows a great simplification in the modelling and a great reduction in the computation time when calculating the non-linear mode shapes, the associated non-linear frequencies, and the non-linear bending stress patterns, for a reasonable range of vibration amplitudes and plate aspect ratios. In the present work, concerned with symmetrically laminated plates, the validity of this assumption has also been examined, via comparison of the non-linear frequency estimates it

leads to, with those obtained by the HFEM, for two symmetrically laminated plates, with different lay-ups and thicknesses. This discussion is presented in sections 4 and 5.

As mentioned in section 3, $A_{16} = A_{26} = 0$ and $D_{16} = D_{26} = 0$ for a plate having a lay-up $(45, -45, 0, -45, 45, -45, 0, 45)_{sym}$ and $A_{16} = A_{26} = 0$ for a plate having a lay-up $(90, -45, 45, 0)_{sym}$.

2.2. NUMERICAL MODEL FOR THE NON-LINEAR MODE SHAPES AND RESONANCE FREQUENCY OF FULLY CLAMPED RECTANGULAR SYMMETRICALLY LAMINATED PLATES

Previous studies concerned with beams and isotropic plates [42, 43, 47] have shown that harmonic distortion of the non-linear response of a harmonically excited structure occurs at large flexural vibration amplitudes. In the present work, experimental measurements and separation of the first and second harmonics of the plate response at various measuring points have shown a second-harmonic spatial distribution similar to that mentioned in reference [42] in the isotropic plate case (see Figure 9 of section 5.3). To take into account this effect, the transverse displacement function W may be written as in references [40, 42] in the form of a double series,

$$W = \{A_k\}^{\mathrm{T}}\{W\} \sin k\omega t, \tag{13}$$

where $\{A_k\}^{\mathrm{T}} = [a_1^k, a_2^k, \ldots, a_n^k\}$ is the matrix of coefficients corresponding to the kth harmonic, $\{W\}^{\mathrm{T}} = [w_1, w_2, \ldots, w_n]$ is the basic spatial functions matrix, k is the number of harmonics taken into account, and the usual summation convention on the repeated index k is used. Examination of this effect would have led to a too large set of non-linear algebraic equations, i.e., $k \times n - 1$; and exceeded the scope of the present work concerned mainly with the dependence of the response first-harmonic component on the amplitude of vibration and its consequences on the frequency of vibration and the associated bending stress patterns. The numerical results for orthotropic rectangular plates from reference [54] indicated that there is only a very little difference between using the first term and using the first two terms in the truncated times series of equation (13). So, only the term corresponding to $k = 1$ has been taken into account, which has led to the displacement function series reduced, as in reference [2], to only one harmonic: i.e.,

$$W = a_i w_i(x, y) \sin \omega t. \tag{14}$$

Here the usual summation convention for the repeated indexes i is used. i is summed over the range 1 to n, with n being the number of basic functions considered. Discretization of the strain and kinetic energy expressions can be carried out leading to

$$V_b = \tfrac{1}{2} a_i a_j k_{ij} \sin^2 \omega t, \quad V_a = \tfrac{1}{2} a_i a_j a_k a_l b_{ijkl} \sin^4 \omega t, \quad T = \tfrac{1}{2} a_i a_j \omega^2 m_{ij} \cos^2 \omega t, \tag{15}$$

in which m_{ij}, k_{ij} and b_{ijkl} are the mass tensor, the rigidity tensor and the geometrical non-linearity tensor respectively. The expressions for these tensors are

$$k_{ij} = \frac{aH^5 E}{b^3} k_{ij}^*, \quad b_{ijkl} = \frac{aH^5 E}{b^3} b_{ijkl}^*, \quad m_{ij} = \rho H^3 a b m_{ij}^*, \tag{16–18}$$

where the non-dimensional tensors m^*_{ij}, k^*_{ij} and b^*_{ijkl} are given in terms of integrals of the non-dimensional basic functions w^*_i's, defined in Appendix A, and their first and second partial derivatives, by

$$m^*_{ij} = \int_{S^*} w^*_i w^*_j \, \mathrm{d}x^* \, \mathrm{d}y^*, \tag{19}$$

$$\begin{aligned} k^*_{ij} = \int_{S^*} \Bigg\{ & D^*_{11}\alpha^4 \left[\frac{\partial^2 w^*_i}{\partial x^{*^2}} \frac{\partial^2 w^*_j}{\partial x^{*^2}} \right] + D^*_{22} \left[\frac{\partial^2 w^*_i}{\partial y^{*^2}} \frac{\partial^2 w^*_j}{\partial y^{*^2}} \right] \\ & + D^*_{12}\alpha^2 \left[\frac{\partial^2 w^*_i}{\partial x^{*^2}} \frac{\partial^2 w^*_j}{\partial y^{*^2}} + \frac{\partial^2 w^*_i}{\partial y^{*^2}} \frac{\partial^2 w^*_j}{\partial x^{*^2}} \right] + 2D^*_{16}\alpha^3 \left[\frac{\partial^2 w^*_i}{\partial x^{*^2}} \frac{\partial^2 w^*_j}{\partial x^* y^*} + \frac{\partial^2 w^*_i}{\partial x^* y^*} \frac{\partial^2 w^*_j}{\partial x^{*^2}} \right] \\ & + 2D^*_{26}\alpha \left[\frac{\partial^2 w^*_i}{\partial y^{*^2}} \frac{\partial^2 w^*_j}{\partial x^* y^*} + \frac{\partial^2 w^*_i}{\partial x^* y^*} \frac{\partial^2 w^*_j}{\partial y^{*^2}} \right] + 4D^*_{66}\alpha^4 \left[\frac{\partial^2 w^*_i}{\partial x^* y^*} \frac{\partial^2 w^*_j}{\partial x^* y^*} \right] \Bigg\} \mathrm{d}S^*. \end{aligned} \tag{20}$$

In the third, fourth and fifth terms between brackets in the above expression, pairs of terms obtained by interchanging i and j were used instead of one term. This was done as in reference [17] in order to make the k^*_{ij} tensor symmetric, as required by the theory [17], which does not change the sum $\frac{1}{2}a_i a_j k^*_{ij}$ corresponding to the bending strain energy V_a. Also,

$$\begin{aligned} b^*_{ijkl} = \int_{S^*} \Bigg\{ & \frac{A^*_{11}}{4}\alpha^4 \left[\frac{\partial w^*_i}{\partial x^*} \frac{\partial w^*_j}{\partial x^*} \frac{\partial w^*_k}{\partial x^*} \frac{\partial w^*_l}{\partial x^*} \right] + \frac{A^*_{22}}{4} \left[\frac{\partial w^*_i}{\partial y^*} \frac{\partial w^*_j}{\partial y^*} \frac{\partial w^*_k}{\partial y^*} \frac{\partial w^*_l}{\partial y^*} \right] \\ & + \left[\frac{A^*_{12}}{4} + \frac{A^*_{66}}{2} \right] \alpha^2 \left\{ \left[\frac{\partial w^*_i}{\partial y^*} \frac{\partial w^*_j}{\partial y^*} \frac{\partial w^*_k}{\partial x^*} \frac{\partial w^*_l}{\partial x^*} \right] + \left[\frac{\partial w^*_i}{\partial x^*} \frac{\partial w^*_j}{\partial x^*} \frac{\partial w^*_k}{\partial y^*} \frac{\partial w^*_l}{\partial y^*} \right] \right\} \\ & + \frac{A^*_{16}}{4}\alpha^3 \left\{ \left[\frac{\partial w^*_i}{\partial x^*} \frac{\partial w^*_j}{\partial x^*} \frac{\partial w^*_k}{\partial x^*} \frac{\partial w^*_l}{\partial y^*} \right] + \left[\frac{\partial w^*_i}{\partial x^*} \frac{\partial w^*_j}{\partial x^*} \frac{\partial w^*_k}{\partial y^*} \frac{\partial w^*_l}{\partial x^*} \right] \right\} \\ & + \frac{A^*_{26}}{2}\alpha \left\{ \left[\frac{\partial w^*_i}{\partial x^*} \frac{\partial w^*_j}{\partial y^*} \frac{\partial w^*_k}{\partial y^*} \frac{\partial w^*_l}{\partial y^*} \right] + \left[\frac{\partial w^*_i}{\partial y^*} \frac{\partial w^*_j}{\partial x^*} \frac{\partial w^*_k}{\partial y^*} \frac{\partial w^*_l}{\partial y^*} \right] \right\} \Bigg\} \mathrm{d}S^*. \end{aligned} \tag{21}$$

As mentioned above for k^*_{ij}, the last three terms have been written twice, with interchanging appropriate indices in each case, in order to obtain a b^*_{ijkl} tensor fulfilling the symmetry requirements assumed in the derivation procedure (see Appendix A): $b^*_{ijkl} = b^*_{klij}$ and $b^*_{ijkl} = b^*_{jikl}$, which does not change the sum $\frac{1}{2}a_i a_j a_k a_l b^*_{ijkl}$ giving the axial strain energy V_a. An illustration of this procedure is given in Appendix A.

In equations (20) and (21), $A^*_{ij} = (A_{ij}/HE)$ and $D^*_{ij} = (D_{ij}/H^3E)$, in which H is the plate thickness and E is a reference Young's modulus, whose numerical value was taken as 7×10^{10} N/m, which is a typical value for aluminium alloys.

Upon neglecting energy dissipation, the equation of motion derived from Hamilton's principle is

$$\delta \int_0^{2\pi} (V - T) = 0, \tag{22}$$

where $V = V_a + V_b$. Insertion of equation (15) into equation (22), and derivation with respect to the unknown constants a_i, leads to the following set of non-linear algebraic equations (23), as shown in Appendix A:

$$3a_i a_j a_k b^*_{ijkl} + 2a_j k^*_{ir} - 2a_i \omega^{*^2} m^*_{ir} = 0, \quad i = 1, \ldots, n. \tag{23}$$

These have to be solved numerically.

To complete the formulation, the procedure developed in reference [17] is adopted to obtain the first non-linear mode. As no dissipation is considered here, a supplementary equation can be obtained by applying the principle of conservation of energy, which can be written as

$$V_{max} = T_{max}. \tag{24}$$

This leads to the equation

$$\omega^{*^2} = \frac{a_i a_j k^*_{ij} + a_i a_j a_k a_l b^*_{ijkl}}{a_i a_j m^*_{ij}}. \tag{25}$$

This expression for ω^{*^2} is substituted into equation (23) to obtain a system of n non-linear algebraic equations leading to the contribution coefficients a_i, $i = 1$ to n.

ω and ω^* are the non-linear frequency and non-dimensional non-linear frequency parameters related by

$$\omega^2 = (H^2 E/\rho b^4)\omega^{*^2}. \tag{26}$$

To obtain the first non-linear mode shape of the plate considered, the contribution of the first basic function is first fixed and the other basic functions contributions are calculated via the numerical solutions of the remaining $(n - 1)$ non-linear algebraic equations.

2.3. BENDING STRESS ANALYSIS FOR FULLY CLAMPED SYMMETRICALLY LAMINATED RECTANGULAR PLATES

Many analytical and numerical methods used to model the geometrically non-linear vibration of plates and beams considered transverse displacement only [38]. It is well known that the estimation of the total non-linear stress must include the in-plane displacements U and V. But, the scope of the present work permitted only consideration of bending stress, which allows only a qualitative understanding of the non-linearity effects. The in-plane membrane stresses are the subject of the next paper, in progress, which will be submitted for publication.

The maximum bending strains ε_{xb} and ε_{yb} obtained for $z = H/2$ are given by

$$\varepsilon_{xb} = \left(\frac{H}{2}\right)\left(\frac{\partial^2 W}{\partial x^2}\right), \quad \varepsilon_{yb} = \left(\frac{H}{2}\right)\left(\frac{\partial^2 W}{\partial y^2}\right). \tag{27, 28}$$

For the plate considered here (see section 3), and for $z = H/2$ which corresponds to a layer for which $\theta = 90^\circ$, one has $Q_{16} = Q_{26} = 0$. By using the stress–strain relationship (5), the

stresses at $z = H/2$ can be obtained as

$$\sigma_{xb} = \frac{HQ_{11}}{2}\frac{\partial^2 W}{\partial x^2} + \frac{HQ_{12}}{2}\frac{\partial^2 w}{\partial y^2}, \qquad \sigma_{yb} = \frac{HQ_{12}}{2}\frac{\partial^2 W}{\partial x^2} + \frac{HQ_{22}}{2}\frac{\partial^2 w}{\partial y^2}. \tag{29, 30}$$

In terms of the non-dimensional parameters defined in the previous work [17], non-dimensional bending stresses σ^*_{xb} and σ^*_{yb} can be defined by

$$\sigma^*_{xb} = \alpha^2\beta\left(\frac{\partial^2 w^*}{\partial x^{*^2}}\right) + \left(\frac{\partial^2 w^*}{\partial y^{*^2}}\right), \qquad \sigma^*_{yb} = \alpha^2\left(\frac{\partial^2 w^*}{\partial x^{*^2}}\right) + \gamma\left(\frac{\partial^2 w^*}{\partial y^{*^2}}\right), \tag{31, 32}$$

where $\alpha = b/a$, $\beta = Q_{11}/Q_{12}$ and $\gamma = Q_{22}/Q_{12}$. The relationship between the dimensional and non-dimensional stresses is

$$\sigma = (Q_{12}H^2/2b^2)\sigma^*, \tag{33}$$

which is valid for both dimensional and non-dimensional pairs of stresses defined by equations (29)–(32).

3. THE PLATE TESTED AND EXPERIMENTAL DETAILS

Quasi-isotropic laminates are made of three or more lamina of identical thickness and material with equal angles between each adjacent lamina. Thus, if the total number of laminas is n, the orientation angles of the laminas are at increments π/n. The resulting laminate exhibits an in-plane isotropic elastic behaviour in the xy plane. However, its strength properties may still vary with the direction of loading. A very common and widely used quasi-isotropic symmetrical stacking sequence is $(90^\circ, -45^\circ, 45^\circ, 0^\circ)_{sym}$ [53]. There is a very practical reason for quasi-isotropic laminates being considered to be isotropic like conventional materials. A direct substitution of this laminate for the conventional material can be done without hesitation because this substitution yields a component which is not substantially different from that made of conventional materials. For example, the quasi-isotropic Young's modulus of T300/5208 (Graphite/Epoxy material where: $E_x = 181\,\text{GPa}$, $E_y = 10{\cdot}3\,\text{GPa}$, $v_x = 0{\cdot}28$ m $E_s = 7{\cdot}17\,\text{GPa}$, $v_f = 0{\cdot}70$ and specific gravity = 1·6) is equal to the Young's modulus of aluminium. But there is a minimum of 40% savings in weight. When directionality in construction is judiciously added, the advantages of composites are overwhelming [55].

Two graphite/epoxy symmetrically rectangular laminated plates are considered here. Their geometrical properties are defined in Tables 1 and 2. Plate 1 is a specially orthotropic laminated plate, which means that its bending and twisting stiffnesses are uncoupled. Also, as in symmetric laminates, the in-plane and bending stiffnesses are uncoupled [27]. For plate 2, which is a symmetrically laminated plate, the values of the stiffnesses A_{16} and A_{26} are zero [53].

Measurements were carried out on a $(90^\circ, -45^\circ, 45^\circ, 0^\circ)_{sym}$ carbon fibre-reinforced plastic plate made of high tensile surface-treated carbon fibre XAS and epoxy resin 914C with 60% fibre volume fraction. The overall dimensions of the plate were 586×424 mm and the dimensions within the clamped edges were 480×320 mm (aspect ratio $\alpha = 2/3$), dimensions of the clamps and the clamping conditions were identical to those adopted in

TABLE 1

Geometric properties of the plates

Plate	Number of layers	Orientation of principal axes	a (mm)	b (mm)	H (mm)
1	16	$(45, -45, 0, -45, 45, -45, 0, 45)_{sym}$	300	150	2·72
2	8	$(90, -45, 45, 0)_{sym}$	480	320	1

TABLE 2

Material properties of the plates

Plate	E_x(Gpa)	E_y (Gpa)	G_{xy} (Gpa)	v_{xy}	ρ (kg/m^3)
1	173	7·2	3·76	0·29	1540
2	120·5	9·63	3·58	0·32	1540

reference [3]. The thickness is $H = 1$ mm and the elastic properties of the laminate were calculated by using the Engineering Science data unit (ESDU) programs [56].

The plate was harmonically excited by a coil and magnet exciter in the region of its first resonance determined by frequency response tests. For the first non-linear mode shape measurements, the excitation point was chosen to be at the middle of the plate. The electrodynamic exciter imposed no added stiffness and little additional mass on the structure. In order not to load the plate with a response measurement transducer, a non-contacting optical vibration transducer (OVT), similar to that mentioned in references [47, 57], was used for measuring the non-linear dynamic response along sections across the plate area. The response measurements and separation of harmonics were carried out using a B&K 2032 analyzer. Instrumentation used in the experimental work is illustrated in Figure 3. The experimental measurements are presented in section 5.2 and compared to numerical results.

4. CHOICE OF THE CONTRIBUTING BASIC FUNCTIONS AND ANALYSIS OF CONVERGENCE OF THE SERIES EXPANSION

4.1. INTRODUCTION

Consider the fully clamped rectangular CFRP symmetrically laminated plate, shown in Figure 1. The plate deflections in the x and y directions were represented by clamped–clamped beam functions defined in Appendix A. These functions, which satisfy all the fully clamped theoretical boundary conditions, i.e., zero displacement and zero slope along the four plate edges, have been used and shown to be appropriate in previous studies on the vibration of fully clamped rectangular plates [1, 2, 15, 58, 59]. In this paper, the index i used in the series expansion of the plate deflection function W, i.e., equation (14), is replaced by a double index ij,

$$w_i(x, y) = w_{ij}(x, y), \tag{34}$$

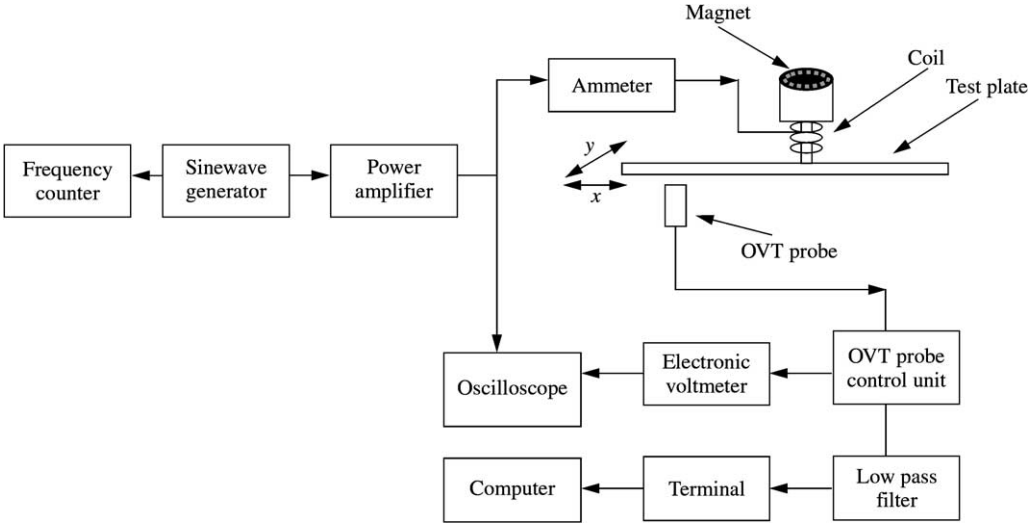

Figure 3. Instrumentation layout for mode shape measurements using digital data acquisition.

In which w_{ij} is the product of the ith and jth clamped–clamped beam functions. The analytical expressions and the shapes of the clamped–clamped beam functions are given in reference [2]. To obtain the first non-linear mode shape of a fully clamped rectangular CFRP symmetrically laminated plate, a judicious choice of basic functions had to be made through a linear analysis and a convergence study, as discussed below. This has led to calculations involving each time a given number of functions. For example, when using 25 basic functions, a set of 24 non-linear algebraic equations had to be solved numerically for various values of the amplitude of vibration and plate aspect ratios. The Harwell library routine NS01A was used, which is based on a hybrid method combining the steepest descent and Newton's methods and consequently exploits the advantages of both methods [60]. A step procedure, similar to that described in reference [1], was adopted for ensuring rapid convergence when varying the amplitude, which allowed solutions to be obtained with quite a reasonable number of iterations (an average of 96 iterations was needed for 17 equations and 160 iterations for 25 equations).

Previous linear and non-linear studies carried out for fully clamped rectangular isotropic plates have shown that plate functions contributing significantly to a given non-linear mode shape are those which contribute significantly to be corresponding linear mode shape [2, 5, 59, 61]. In a previous study carried out on the non-linear vibration of fully clamped rectangular laminated plates, it was assumed, based on the analogy with the isotropic case, that the fundamental CFRP plate non-linear mode shape could be well estimated by using nine plate functions symmetric in both the length and width directions [3]. This has led to a set of eight non-linear algebraic equations, which have been solved numerically for various values of the displacement amplitude of vibration and the plate aspect ratio.

To start the present work, a linear analysis was made by using 6×6 plate basic functions obtained as products of the first six clamped–clamped x-beam functions by the first six clamped–clamped y-beam functions in order to determine the basic functions which contribute significantly to the fundamental linear mode shape, because they were expected to be also the useful ones in the non-linear case. Then, to confirm the validity of such an assumption, based on the analogy with the previous studies carried out by using the present model [2, 5, 45], calculations have been performed in the non-linear case by using 5×5

TABLE 3

First linear mode shape of a fully clamped CFRP rectangular plate 2 ($\alpha = 0{\cdot}6$): typical numerical results obtained with 36 basic functions

	ω_l^*	7·6264			
1	a_{11}	1	19	a_{41}	−1·060938E − 10
2	a_{12}	−1·298783E − 10	20	a_{42}	− 5·989084E − 03
3	a_{13}	2·561815E − 03	21	a_{43}	1·799209E − 12
4	a_{14}	− 4·480797E − 12	22	a_{44}	− 4·104451E − 04
5	a_{15}	3·322017E − 04	23	a_{45}	4·697111E − 13
6	a_{16}	5·408843E − 11	24	a_{46}	− 7·526413E − 05
7	a_{21}	−1·493365E − 09	25	a_{51}	8·747784E − 03
8	a_{22}	−1·757448E − 02	26	a_{52}	1·691052E − 11
9	a_{23}	− 9·066346E − 12	27	a_{53}	− 6.794652E − 04
10	a_{24}	− 9·011867E − 04	28	a_{54}	1·751740E − 12
11	a_{25}	− 8·752992E − 13	29	a_{55}	− 1·398728E − 04
12	a_{26}	− 1·528316E − 04	30	a_{56}	3·309399E − 13
13	a_{31}	4·966702E − 02	31	a_{61}	7·279856E − 11
14	a_{32}	3·541135E − 11	32	a_{62}	− 2·564118E − 03
15	a_{33}	− 8·248961E − 04	33	a_{63}	− 1·850183E − 13
16	a_{34}	2·665265E − 12	34	a_{64}	− 2·011116E − 04
17	a_{35}	−1·333734E − 04	35	a_{65}	8·230034E − 14
18	a_{36}	2·631115E − 12	36	a_{66}	− 3·337539E − 05

basic functions in order to confirm that the omitted functions have negligible contributions, as discussed below.

4.2. RESULTS OF LINEAR ANALYSIS

If the non-linear term $3a_i a_j a_k b^*_{ijkl}$ is neglected in equation (23), the classical linear modal analysis free vibration equation is obtained,

$$a_i k^*_{ir} = a_i \omega^{*^2} m^*_{ir}, \quad r = 1, \ldots, n, \tag{35}$$

which has to be solved to obtain the plate linear mode shapes and resonance frequencies. Calculation was made by using 36 basic functions obtained as products of the first six clamped–clamped beam functions, leading to square mass and rigidity matrices of dimension 36. Eigenvalue problem (35) has been solved by using MATLAB software. An example of the numerical results obtained for a plate 2 having an aspect ratio $\alpha = 0{\cdot}6$ is summarized in Table 3. It can be seen that only 18 functions corresponding to three symmetric functions in the x direction and three symmetric beam functions in the y direction, and three antisymmetric beam functions in the x direction and three antisymmetric beam functions in the y direction, contribute significantly to the first linear mode of the fully clamped rectangular CFRP symmetrically laminated plate. The ratio of the highest contribution of the omitted functions to the smallest contribution of the significant functions (a_{21}/a_{66}) is about (4.5×10^{-5}).

In order to verify the accuracy of the results obtained in the present work from the solution of equation (35), comparisons have been made with some available results obtained by the HFEM in reference [40]. Table 4 shows the comparison of linear natural frequencies

TABLE 4

Comparison of linear natural frequencies of plate 1 *between results obtained in reference* [40] *and present results*

	ω_{11} (rad/s)	ω_{12}/ω_{11}	ω_{13}/ω_{11}	ω_{14}/ω_{11}	ω_{15}/ω_{11}	ω_{16}/ω_{11}	ω_{17}/ω_{11}	ω_{18}/ω_{11}
HFEM $p_o = 10$	4941·48	1·4773	2·2047	2·4728	3·0309	3·1715	3·8642	4·3788
Present results	4944·3	1·4776	2·2066	2·4737	3·0344	3·1739	3·8761	4·3823
Error (%)	0·05	0·044	0·053	0·057	0·059	0·075	0·3	0·08

TABLE 5

Comparison of linear natural frequencies (rad/s) *of plate* 1 *between results obtained in reference* [40] *and present results*

p_o d.o.f.	5 25	6 36	7 49	10 100	Present results	Average	S.D.
ω_1	4941·817	4941·817	4941·533	4941·484	4944·30	4942·19	1·895
ω_2	7302·876	7300·268	7300·230	7299·848	7306·12	7301·876	2·681
ω_3	10904·63	10904·63	10894·69	10894·44	10910·48	10901·48	7·001
ω_4	12223·93	12220·70	12219·51	12219·32	12230·92	12222·88	4·861
ω_5	14994·59	14979·04	14979·04	14977·37	15003·46	14986·7	11·699

of plate 1 with a maximum difference of 0·3% obtained for the seventh mode shape. In Table 5, the first five natural frequencies of plate 1 are compared with those obtained in reference [40], and a good agreement is found.

4.3. TYPICAL VALUES OBTAINED BY USE OF 25 FUNCTIONS FOR THE NON-LINEAR ANALYSIS

To confirm the good convergence of the series expansion and the validity of use of 18 plate functions mentioned above, the first non-linear plate mode shape has been calculated by using 25 plate functions obtained as the product of the first five beam functions (symmetric and antisymmetric). An example of the numerical results obtained for a plate 2 having an aspect ratio $\alpha = 0{\cdot}6$ and maximum non-dimensional vibration amplitudes w^*_{max} of 0·0485, 0·7067 and 2·3725 corresponding to the assigned contribution functions a_{11} taken equal to 0·02, 0·3 and 1·05, respectively, are listed in Table 6. It can be seen that functions having significant contributions are those expected according to the analysis given above: i.e., a_{11}, a_{13}, a_{15}, a_{22}, a_{24}, a_{26}, a_{31}, a_{33}, a_{35}, a_{42}, a_{44}, a_{46}, a_{51}, a_{53}, a_{55}, a_{62}, a_{64}, a_{66}. The values of their contributions, listed in Table 6 are very close to those corresponding to the same functions in Table 7 in which non-linear results obtained by using only 18 well-chosen plate functions are given. The slight difference is due to the fact that the 25 basic plate functions used do not involve the functions w_{26}, w_{46}, w_{62} w_{64} and w_{66}.

Based on the results of this section, it can be concluded that the first non-linear mode shape of the fully clamped rectangular CFRP symmetrically laminated plate can be obtained with enough accuracy by using the 18 basic plate functions mentioned above. This significantly simplifies the computation effort, since calculations of the non-linearity tensor

TABLE 6

First non-linear mode shape of a fully clamped CFRP *rectangular plate* $2(\alpha = 0{\cdot}6)$: *typical numerical results obtained with* 25 *basic functions* (*obtained as product of the first five clamped–clamped beam functions*)

	W^*_{max} ω^*_{nl}/ω^*_l	0·0485 1·0004	0·7067 1·0635	2·3725 1·5421
1	a_{11}	0·02	0·3	1·05
2	a_{12}	−2·5557E − 12	−4·8115E − 11	−3·3767E − 10
3	a_{13}	5·1954E − 05	2·1815E − 03	3·1552E − 02
4	a_{14}	−9·3837E − 14	−3·1112E − 12	−5·0112E − 11
5	a_{15}	6·7864E − 06	7·0164E − 04	1·6836E − 02
6	a_{21}	−2·8350E − 11	−3·3011E − 10	−7·4654E − 10
7	a_{22}	−3·4858E − 04	−4·2947E − 03	−5·9254E − 03
8	a_{23}	−1·7190E − 13	−3·9571E − 12	−2·9780E − 11
9	a_{24}	−1·7987E − 05	−2·2685E − 04	−1·8128E − 04
10	a_{25}	−2·6406E − 14	−1·2250E − 12	−1·3722E − 11
11	a_{31}	9·8746E − 04	2·5397E − 02	1·5474E − 01
12	a_{32}	6·9685E − 13	2·8432E − 12	−5·0838E − 11
13	a_{33}	−1·5460E − 05	2·6471E − 04	1·3566E − 02
14	a_{34}	4·7720E − 14	9·5164E − 13	4·4398E − 12
15	a_{35}	−2·5792E − 06	−1·7013E − 04	−1·6279E − 03
16	a_{41}	−2·1675E − 12	−3·8562E − 11	−1·2633E − 10
17	a_{42}	−1·1698E − 04	−1·9321E − 03	−3·8021E − 03
18	a_{43}	4·0529E − 14	−8·3772E − 13	−1·2540E − 11
19	a_{44}	−8·1253E − 06	−1·8932E − 04	−8·1591E − 04
20	a_{45}	−1·3196E − 14	2·2359E − 13	−1·0096E − 12
21	a_{51}	1·6466E − 04	4·0533E − 03	3·6258E − 02
22	a_{52}	3·3427E − 13	3·4872E − 12	−1·0548E − 11
23	a_{53}	−1·0659E − 05	−1·4571E − 04	4·3481E − 03
24	a_{54}	4·0049E − 14	5·3569E − 13	2·4752E − 12
25	a_{55}	−2·1874E − 06	−2·7251E − 05	−2·9319E − 04

b^*_{ijkl} involve $36^4 = 1\,679\,616$ terms when using 36 basic plate functions, but only $18^4 = 104\,976$ when using 18 basic plate functions.

4.4. NON-LINEAR ANALYSIS AT SMALL VIBRATION AMPLITUDES FOR THE CFRP PLATE

Numerical results from the non-linear analysis of a CFRP composite plate having aspect ratios $\alpha = 0{\cdot}6$, 0·8 and 1 and values of the maximum non-dimensional vibration amplitudes w^*_{max} of 0·0218, 0·0220 and 0·0222 corresponding to the assigned contribution functions a_{11} taken equal to 0·012 are compared in Table 8 to linear results obtained from the solution of the classical eigenvalue problem (35). It can be seen that both resonance frequencies and contribution coefficients obtained from the non-linear analysis at small vibration amplitude are very close to those obtained from the linear analysis. Consequently, a very good agreement can be noticed between data from a linear model and non-linear model at small deflections. It is worth noting here, from the numerical methods point of view, that a classical eigenvalue problem, solved by using classical numerical methods, such as Jacobi's method, appears here, as has been pointed out when dealing with the first non-linear plate mode shape in reference [2], as a limit of a nonlinear problem, described by a set of non-linear algebraic equations, the solution of which tends to the eigenvalue problem solution when the displacement amplitude tends to zero.

TABLE 7

First non-linear mode shape of a fully clamped CFRP *rectangular plate* 2($\alpha = 0{\cdot}6$): *typical numerical results obtained with* 18 *well chosen basic functions*

	W^*_{max} ω^*_{nl}/ω^*_l	0·0485 1·0003	0·7067 1·0634	2·3725 1·5419
1	a_{11}	0·02	0·3	1·05
2	a_{13}	5·1722E − 05	2·1761E − 03	3·1540E − 02
3	a_{15}	6·8370E − 06	7·0241E − 04	1·6838E − 02
4	a_{22}	− 3·5113E − 04	− 4·3644E − 03	− 6·6699E − 03
5	a_{24}	− 1·8008E − 05	− 2·2747E − 04	− 1·9944E − 04
6	a_{26}	− 3·0640E − 06	− 6·6520E − 05	− 4·6894E − 04
7	a_{31}	9·9790E − 04	2·5538E − 02	1·5483E − 01
8	a_{33}	− 1·6347E − 05	2·4739E − 04	1·3539E − 02
9	a_{35}	− 2·7193E − 06	− 1·7343E − 04	− 1·6504E − 03
10	a_{42}	− 1·1992E − 04	− 2·0196E − 03	− 4·5389E − 03
11	a_{44}	− 8·2392E − 06	− 1·9198E − 04	− 9·6271E − 04
12	a_{46}	− 1·5056E − 06	− 2·4883E − 05	− 1·7123E − 04
13	a_{51}	1·7544E − 04	4·2124E − 03	3·6398E − 02
14	a_{53}	− 1·3613E − 05	− 1·9024E − 04	4·3213E − 03
15	a_{55}	− 2·7910E − 06	− 3·8672E − 05	− 3·3892E − 04
16	a_{62}	− 5·1350E − 05	− 9·2028E − 04	− 2·5585E − 03
17	a_{64}	− 4·0322E − 06	− 9·7614E − 05	− 9·1235E − 04
18	a_{66}	− 6·6954E − 07	− 1·5000E − 05	− 1·4482E − 04

TABLE 8

Comparison of contribution coefficients to the first mode shape of a fully clamped CFRP *rectangular plate* 2 *for* $\alpha = 0{\cdot}6$, 0·8 *and* 1; (*a*) *linear results calculated here*; (*b*) *present results obtained from non-linear analysis*

	$\alpha = 0{\cdot}6$ and $W^* = 0{\cdot}0218$		$\alpha = 0{\cdot}8$ and $W^* = 0{\cdot}0220$		$\alpha = 1$ and $W^* = 0{\cdot}0222$	
	(a)	(b)	(a)	(b)	(a)	(b)
ω^*	7·6264	7·6269	8·1331	8·1334	8·917	8·918
a_{11}	1	1	1	1	1	1
a_{13}	0·0025618	0·0025707	0·004467	0·004473	0·0068042	0·0068116
a_{15}	0·0003322	0·0003376	0·000589	0·000591	0·0009121	0·0009140
a_{22}	− 0·0175745	− 0·0175372	− 0·024249	− 0·024243	− 0·0299748	− 0·0299686
a_{24}	− 0·0009012	− 0·0008950	− 0·001471	− 0·001471	− 0·0021798	− 0·0021797
a_{26}	− 0·0001528	− 0·0001540	− 0·000264	− 0·000264	− 0·0004165	− 0·0004166
a_{31}	0·0496670	0·0501311	0·033337	0·033367	0·0229685	0·0229886
a_{33}	− 0·0008249	− 0·0008307	− 0·001449	− 0·001447	− 0·0018566	− 0·0018538
a_{35}	− 0·0001334	− 0·0001346	− 0·000278	− 0·000278	− 0·0004302	− 0·0004309
a_{42}	− 0·0059891	− 0·0060319	− 0·006116	− 0·006117	− 0·0056798	− 0·0056795
a_{44}	− 0·0004105	− 0·0004264	− 0·000526	− 0·000527	− 0·0005938	− 0·0005944
a_{46}	− 0·0000753	− 0·0000719	− 0·000103	− 0·000103	− 0·0001222	− 0·0001222
a_{51}	0·0087478	0·0081772	0·005070	0·005076	0·0032064	0·0032126
a_{53}	− 0·0006795	− 0·0007065	− 0·000813	− 0·000814	− 0·0007779	− 0·0007789
a_{55}	− 0·0001399	− 0·0001487	− 0·000215	− 0·000215	− 0·0002618	− 0·0002617
a_{62}	− 0·0025641	− 0·0025325	− 0·002055	− 0·002056	− 0·0016062	− 0·0016069
a_{64}	− 0·0002011	− 0·0002031	− 0·000187	− 0·000187	− 0·0001686	− 0·0001686
a_{66}	− 0·0000334	− 0·0000351	− 0·000025	− 0·000025	− 0·0000127	− 0·0000127

TABLE 9

Comparison of non-linear frequency ratio ω_{nl}^*/ω_l^* *of plate 2 for* $\alpha = 2/3$, ($a = 0{\cdot}48\,m$, $b = 0{\cdot}32\,m$) *between results obtained in reference* [38] *associated with the fundamental non-linear mode shape and present results*

A_m/H	HFEM $p_i = p_o = 5$	Present results	Error (%)
0·2	1·0058	1·0054	0·039
0·4	1·0232	1·0214	0·0017
0·6	1·0516	1·0475	0·0039
0·8	1·0903	1·0826	0·0070
1·0	1·1382	1·1267	0·0101
1·2	1·1941	1·1759	0·0152

5. FIRST NON-LINEAR MODE SHAPE

5.1. COMPARISON OF THE FREQUENCY AMPLITUDE DEPENDENCE CALCULATED VIA THE PRESENT THEORY WITH PREVIOUS RESULTS

In order to estimate the accuracy of the results obtained by the present theory, and the effects of the approximations adopted, a comparison has been made with previous results, for large vibration amplitudes, based on the HFEM presented in reference [40].

Table 9 shows the comparison of the non-linear frequency ratios obtained in reference [38], with the present results for the fully clamped CFRP rectangular plate 2. The ω_{nl}^*/ω_l^* calculated from the present model is very close to the results produced by the HFEM with the in-plane and out-of-plane shape functions $p_i = p_o = 5$ respectively. The error does not exceed 1·01% in the non-linear frequency ratio ω_{nl}^*/ω_l^* estimates for amplitudes up to 1 time the plate thickness. Figures 4–7 show a reasonable agreement between results given in reference [40] and the present results for the fully clamped CFRP rectangular plate 1. This good agreement, added to the reasons mentioned in section 2.1, shows that the assumption for neglecting U and V can lead to reasonable estimation of the first non-linear mode of fully clamped symmetrically laminated rectangular plates.

The good agreement of the results shown in Table 9 and Figures 4–7 above indicate that the model used in this work can be applied to geometrically non-linear analysis of laminated plates with good accuracy.

5.2. GENERAL PRESENTATION OF NUMERICAL RESULTS

Numerical results for a CFRP plate 2 corresponding to assigned values of a_{11} varying from 0·05 to 1·05 corresponding to a maximum displacement amplitude to thickness ratio varying from 0·1216 to 2·5174, obtained at $(x^*, y^*) = (0{\cdot}5, 0{\cdot}5)$, and $\alpha = 2/3$, 1 and 3/2 are summarized in Tables 10–12. In each table, a_{ij} represents the contribution of the basic function obtained as product of the ith and the jth x and y clamped–clamped basic functions. w_{max}^* is the maximum non-dimensional amplitude and ω_{nl}^*/ω_l^* is the ratio of the non-linear non-dimensional frequency parameter defined in equation (25) to the linear non-dimensional frequency parameter obtained by diagonalization of the linear system.

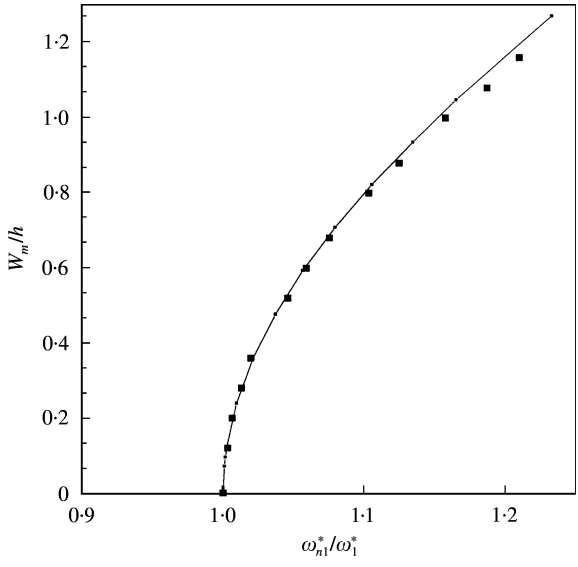

Figure 4. Comparison of backbone curve obtained by present results (—·—) and that published in reference [40] (■, read from graph). Plate 1. (a) $(x^*, y^*) = (0{\cdot}5, 0{\cdot}5)$.

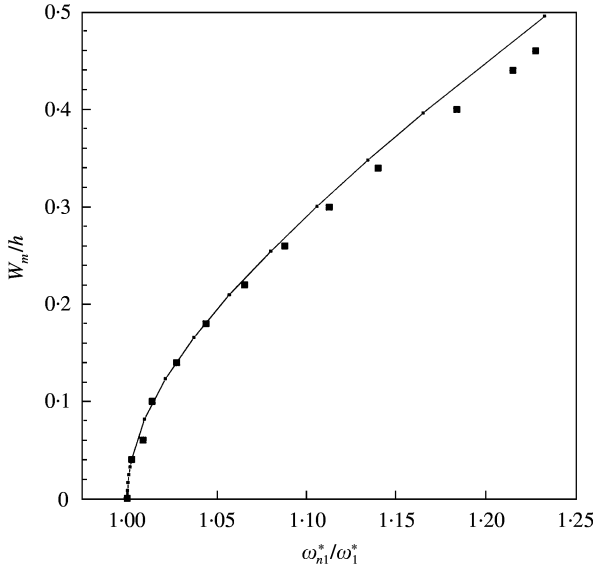

Figure 5. Comparison of backbone curve obtained by present results (—·—) and that published in reference [40] (■, read from graph). Plate 1. (a) $(x^*, y^*) = (0{\cdot}75, 0{\cdot}75)$.

5.3. AMPLITUDE DEPENDENCE OF THE FUNDAMENTAL MODE SHAPE AND COMPARISON WITH EXPERIMENTAL RESULTS FOR A FULLY CLAMPED CFRP RECTANGULAR PLATE 2

The theoretical model involves various approximations, such as the assumption of harmonic motion, the separation of the time and space functions, the neglect of U and V, and integration over the range $[0, 2\pi/\omega]$ when applying Hamilton's principle (which has

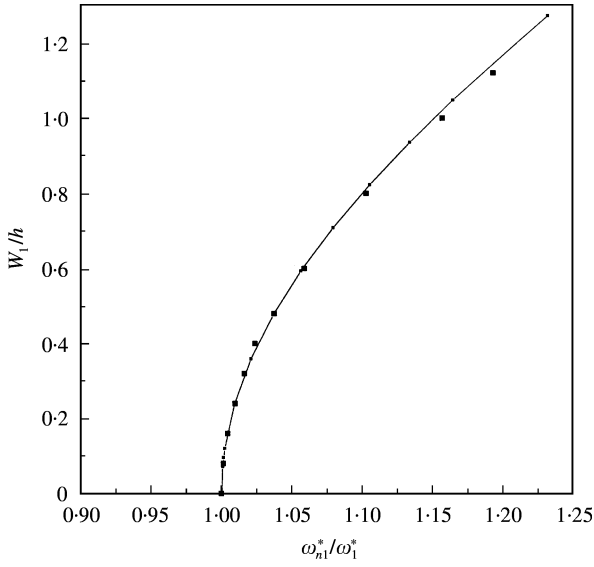

Figure 6. Comparison of backbone curve obtained by present results (—·—) and that published in reference [40] (■, read from graph), with $p_i = 6$ and $p_o = 5$, 6 and 7. Plate 1. (a) $(x^*, y^*) = (0{\cdot}5, 0{\cdot}5)$.

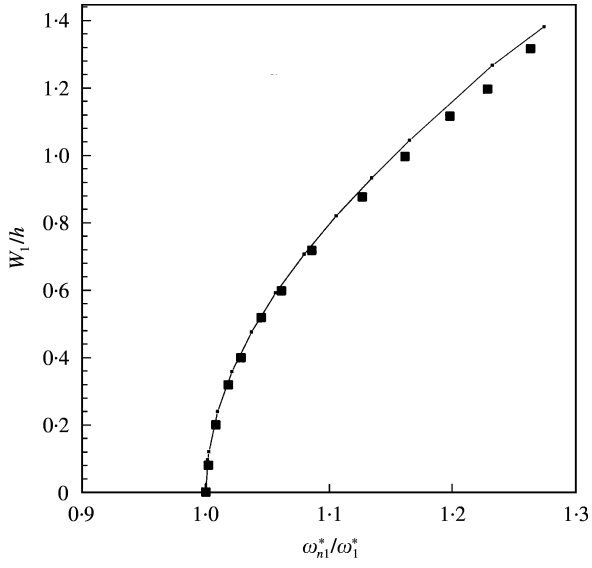

Figure 7. Comparison of backbone curve obtained by present results (—·—) and that published in reference [40] (■, read from graph), with $p_o = 6$ and $p_i = 6$, 7, 8 and 10. Plate 1. (a) $(x^*, y^*) = (0{\cdot}5, 0{\cdot}5)$.

been shown in reference [44] to be equivalent to applying the Harmonic Balance Method). Also, the experimental investigations involve many sources of uncertainty, such as the clamped boundaries which cannot be perfectly achieved, as discussed in reference [5], the effect of the added mass of the exciter; etc. All of the above reasons make it unrealistic to attempt a very accurate comparison between theoretical and experimental numerical values. Also, use of a coil and a magnet to excite a fully clamped panel limits considerably

TABLE 10

Contribution coefficients to the first non-linear mode shape of a fully clamped CFRP *rectangular plate* 2, $\alpha = 2/3$

W^*_{max}	ω^*_{nl}/ω^*_l	a_{11}	a_{13}	a_{15}	a_{22}	a_{24}	a_{26}	a_{31}	a_{33}	a_{35}
0·1216	1·0020	0·05	1·6531E−04	2·3508E−05	−9·8654E−04	−5·3439E−05	−9·4079E−06	2·2273E−03	−4·9473E−05	−9·7506E−06
0·2426	1·0079	0·10	3·7788E−04	6·4809E−05	−1·9382E−03	−1·0542E−04	−1·9587E−05	4·7830E−03	−8·2397E−05	−2·4431E−05
0·3625	1·0176	0·15	6·8062E−04	1·4090E−04	−2·8261E−03	−1·5463E−04	−3·1218E−05	7·9250E−03	−8·2513E−05	−4·8298E−05
0·5980	1·0471	0·25	1·6911E−03	4·5808E−04	−4·3441E−03	−2·4070E−04	−6·0785E−05	1·6452E−02	7·6879E−05	−1·3499E−04
0·8285	1·0884	0·35	3·3864E−03	1·0782E−03	−5·4940E−03	−3·0646E−04	−1·0030E−04	2·7843E−02	5·3716E−04	−2·8124E−04
1·0556	1·1392	0·45	5·8459E−03	2·0742E−03	−6·3162E−03	−3·5054E−04	−1·4966E−04	4·1315E−02	1·3777E−03	−4·8459E−04
1·2818	1·1978	0·55	9·0679E−03	3·4901E−03	−6·8768E−03	−3·7404E−04	−2·0728E−04	5·6024E−02	2·6451E−03	−7·3491E−04
1·5105	1·2626	0·65	1·2997E−02	5·3439E−03	−7·2386E−03	−3·7940E−04	−2·7083E−04	7·1359E−02	4·3563E−03	−1·0181E−03
1·7333	1·3325	0·75	1·7548E−02	7·6317E−03	−7·4530E−03	−3·6976E−04	−3·3783E−04	8·6953E−02	6·5034E−03	−1·3185E−03
1·9597	1·4065	0·85	2·2624E−02	1·0334E−02	−7·5597E−03	−3·4848E−04	−4·0591E−04	1·0261E−01	9·0609E−03	−1·6201E−03
2·1869	1·4839	0·95	2·8128E−02	1·3419E−02	−7·5879E−03	−3·1884E−04	−4·7309E−04	1·1824E−01	1·1992E−02	−1·9079E−03
2·4146	1·5641	1·05	3·3976E−02	1·6850E−02	−7·5594E−03	−2·8381E−04	−5·3774E−04	1·3381E−01	1·5253E−02	−2·1692E−03

W^*_{max}	ω^*_{nl}/ω^*_l	a_{42}	a_{44}	a_{46}	a_{51}	a_{53}	a_{55}	a_{62}	a_{64}	a_{66}
0·1216	1·0020	−3·0777E−04	−2·3277E−05	−4·2721E−06	3·6874E−04	−3·7942E−05	−8·2341E−06	−1·2090E−04	−1·0092E−05	−1·6087E−06
0·2426	1·0079	−6·2362E−04	−4·9625E−05	−8·5286E−06	7·8410E−04	−7·8740E−05	−1·5790E−05	−2·4736E−04	−2·1120E−05	−3·4147E−06
0·3625	1·0176	−9·5173E−04	−8·1462E−05	−1·2782E−05	1·2911E−03	−1·2344E−04	−2·2320E−05	−3·8358E−04	−3·4121E−05	−5·5827E−06
0·5980	1·0471	−1·6340E−03	−1·6619E−04	−2·1530E−05	2·7324E−03	−2·1467E−04	−3·3168E−05	−6·9085E−04	−7·0575E−05	−1·1451E−05
0·8285	1·0884	−2·2984E−03	−2·7787E−04	−3·1237E−05	4·8946E−03	−2·6953E−04	−4·4878E−05	−1·0315E−03	−1·2729E−04	−1·9869E−05
1·0556	1·1392	−2·8805E−03	−4·0891E−04	−4·2598E−05	7·7967E−03	−2·3156E−04	−6·0717E−05	−1·3727E−03	−2·0743E−04	−3·1398E−05
1·2818	1·1978	−3·3453E−03	−5·5054E−04	−5·5975E−05	1·1327E−02	−5·4371E−05	−7·9637E−05	−1·6819E−03	−3·0874E−04	−4·6565E−05
1·5105	1·2626	−3·6882E−03	−6·9538E−04	−7·1420E−05	1·5330E−02	2·8992E−04	−9·6832E−05	−1·9385E−03	−4·2553E−04	−6·5679E−05
1·7333	1·3325	−3·9223E−03	−8·3776E−04	−8·8791E−05	1·9658E−02	8·1249E−04	−1·0569E−04	−2·1348E−03	−5·5101E−04	−8·8715E−05
1·9597	1·4065	−4·0671E−03	−9·7351E−04	−1·0784E−04	2·4195E−02	1·5125E−03	−9·9436E−05	−2·2727E−03	−6·7882E−04	−1·1533E−04
2·1869	1·4839	−4·1424E−03	−1·0996E−03	−1·2828E−04	2·8857E−02	2·3814E−03	−7·2138E−05	−2·3591E−03	−8·0373E−04	−1·4496E−04
2·4146	1·5641	−4·1651E−03	−1·2141E−03	−1·4977E−04	3·3587E−02	3·4062E−03	−1·9107E−05	−2·4029E−03	−9·2184E−04	−1·7689E−04

TABLE 11

Contribution coefficients to the first non-linear mode shape of a fully clamped CFRP *rectangular plate* 2, $\alpha = 1$

W^*_{max}	ω^*_{nl}/ω^*_l	a_{11}	a_{13}	a_{15}	a_{22}	a_{24}	a_{26}	a_{31}	a_{33}	a_{35}
0·1231	1·0027	0·05	3·5245E−04	4·8420E−05	−1·4890E−03	−1·0876E−04	−2·1003E−05	1·1811E−03	−8·8474E−05	−2·2451E−05
0·2459	1·0107	0·10	7·7688E−04	1·1361E−04	−2·9218E−03	−2·1616E−04	−4·3053E−05	2·5497E−03	−1·5089E−04	−5·0406E−05
0·3681	1·0237	0·15	1·3384E−03	2·1174E−04	−4·2515E−03	−3·2083E−04	−6·7067E−05	4·2552E−03	−1·6159E−04	−8·8755E−05
0·6103	1·0631	0·25	3·0740E−03	5·6574E−04	−6·4906E−03	−5·1665E−04	−1·2347E−04	8·9719E−03	6·8211E−05	−2·1060E−04
0·8500	1·1173	0·35	5·8316E−03	1·2118E−03	−8·1283E−03	−6·8720E−04	−1·9256E−04	1·5391E−02	7·6636E−04	−4·0272E−04
1·0882	1·1830	0·45	9·7066E−03	2·2216E−03	−9·2346E−03	−8·2723E−04	−2·7309E−04	2·3093E−02	2·0402E−03	−6·6053E−04
1·3257	1·2575	0·55	1·4673E−02	3·6359E−03	−9·9267E−03	−9·3555E−04	−3·6172E−04	3·1602E−02	3·9338E−03	−9·6564E−04
1·5633	1·3389	0·65	2·0633E−02	5·4686E−03	−1·0316E−02	−1·0141E−03	−4·5434E−04	4·0568E−02	6·4395E−03	−1·2922E−03
1·8011	1·4258	0·75	2·7453E−02	7·7112E−03	−1·0490E−02	−1·0666E−03	−5·4703E−04	4·9770E−02	9·5151E−03	−1·6122E−03
2·0394	1·5169	0·85	3·4990E−02	1·0340E−02	−1·0516E−02	−1·0976E−03	−6·3649E−04	5·9085E−02	1·3099E−02	−1·8999E−03
2·2782	1·6115	0·95	4·3107E−02	1·3322E−02	−1·0440E−02	−1·1117E−03	−7·2025E−04	6·8448E−02	1·7123E−02	−2·1338E−03
2·5174	1·7091	1·05	5·1679E−02	1·6620E−02	−1·0296E−02	−1·1129E−03	−7·9665E−04	7·7825E−02	2·1516E−02	−2·2978E−03

W^*_{max}	ω^*_{nl}/ω^*_l	a_{42}	a_{44}	a_{46}	a_{51}	a_{53}	a_{55}	a_{62}	a_{64}	a_{66}
0·1231	1·0027	−2·8346E−04	−3·0687E−05	−6·0890E−06	1·6995E−04	−4·0550E−05	−1·2850E−05	−8·1359E−05	−8·4824E−06	−6·9431E−07
0·2459	1·0107	−5·6345E−04	−6·7155E−05	−1·2055E−05	3·9646E−04	−9·0542E−05	−2·4314E−05	−1·6868E−04	−1·7337E−05	−1·7369E−06
0·3681	1·0237	−8·3547E−04	−1·1420E−04	−1·7834E−05	7·3026E−04	−1·5713E−04	−3·3281E−05	−2·6647E−04	−2·7139E−05	−3·4502E−06
0·6103	1·0631	−1·3323E−03	−2·5103E−04	−2·9011E−05	1·8683E−03	−3·4999E−04	−4·1142E−05	−4·9969E−04	−5·3069E−05	−1·0025E−05
0·8500	1·1173	−1·7295E−03	−4·4699E−04	−4·0699E−05	3·7535E−03	−6·0429E−04	−3·3130E−05	−7·7219E−04	−9·3523E−05	−2·2569E−05
1·0882	1·1830	−2·0045E−03	−6·8994E−04	−5·4459E−05	6·3796E−03	−8·7226E−04	−4·8814E−06	−1·0559E−03	−1·5254E−04	−4·3161E−05
1·3257	1·2575	−2·1631E−03	−9·6125E−04	−7·1591E−05	9·6397E−03	−1·1034E−03	5·1882E−05	−1·3230E−03	−2·2894E−04	−7·3519E−05
1·5633	1·3389	−2·2283E−03	−1·2429E−03	−9·2819E−05	1·3395E−02	−1·2596E−03	1·4831E−04	−1·5552E−03	−3·1781E−04	−1·1451E−04
1·8011	1·4258	−2·2272E−03	−1·5205E−03	−1·1829E−04	1·7516E−02	−1·3184E−03	2·9598E−04	−1·7441E−03	−4·1293E−04	−1·6595E−04
2·0394	1·5169	−2·1832E−03	−1·7834E−03	−1·4767E−04	2·1892E−02	−1·2705E−03	5·0481E−04	−1·8888E−03	−5·0845E−04	−2·2671E−04
2·2782	1·6115	−2·1142E−03	−2·0248E−03	−1·8029E−04	2·6443E−02	−1·1154E−03	7·8200E−04	−1·9926E−03	−5·9974E−04	−2·9502E−04
2·5174	1·7091	−2·0322E−03	−2·2409E−03	−2·1529E−04	3·1106E−02	−8·5901E−04	1·1316E−03	−2·0610E−03	−6·8360E−04	−3·6875E−04

TABLE 12

Contribution coefficients to the first non-linear mode shape of a fully clamped CFRP *rectangular plate* 2, $\alpha = 3/2$

W^*_{max}	ω^*_{nl}/ω^*_l	a_{11}	a_{13}	a_{15}	a_{22}	a_{24}	a_{26}	a_{31}	a_{33}	a_{35}
0·1236	1·0041	0·05	7·4025E−04	1·0195E−04	−1·8539E−03	−2·1094E−04	−4·7032E−05	5·4894E−04	−8·7072E−05	−3·5030E−05
0·2467	1·0163	0·10	1·6369E−03	2·1809E−04	−3·6157E−03	−4·2461E−04	−9·5145E−05	1·2503E−03	−1·4986E−04	−7·4941E−05
0·3691	1·0358	0·15	2·8269E−03	3·6282E−04	−5·2116E−03	−6·4236E−04	−1·4528E−04	2·2235E−03	−1·6255E−04	−1·2353E−04
0·6110	1·0938	0·25	6·4746E−03	7·9590E−04	−7·7564E−03	−1·0855E−03	−2·5400E−04	5·2080E−03	7·0903E−05	−2·5189E−04
0·8493	1·1711	0·35	1·2132E−02	1·5101E−03	−9·4363E−03	−1·5183E−03	−3·7463E−04	9·5249E−03	8·0936E−04	−4·0698E−04
1·0846	1·2620	0·45	1·9846E−02	2·5918E−03	−1·0423E−02	−1·9147E−03	−5·0395E−04	1·4837E−02	2·1714E−03	−5·4457E−04
1·3179	1·3625	0·55	2·9445E−02	4·0943E−03	−1·0924E−02	−2·2582E−03	−6·3614E−04	2·0787E−02	4·1799E−03	−6·0602E−04
1·5498	1·4701	0·65	4·0662E−02	6·0386E−03	−1·1102E−02	−2·5428E−03	−7·6502E−04	2·7112E−02	6·7870E−03	−5·3539E−04
1·7807	1·5832	0·75	5·3207E−02	8·4182E−03	−1·1073E−02	−2·7699E−03	−8·8534E−04	3·3646E−02	9·9086E−03	−2·9041E−04
2·0109	1·7006	0·85	6·6802E−02	1·1207E−02	−1·0913E−02	−2·9443E−03	−9·9338E−04	4·0289E−02	1·3451E−02	1·5353E−04
2·2406	1·8215	0·95	8·1202E−02	1·4367E−02	−1·0670E−02	−3·0724E−03	−1·0870E−03	4·6983E−02	1·7324E−02	8·0420E−04
2·4700	1·9455	1·05	9·6203E−02	1·7853E−02	−1·0377E−02	−3·1609E−03	−1·1654E−03	5·3693E−02	2·1451E−02	1·6561E−03

W^*_{max}	ω^*_{nl}/ω^*_l	a_{42}	a_{44}	a_{46}	a_{51}	a_{53}	a_{55}	a_{62}	a_{64}	a_{66}
0·1236	1·0041	−2·0413E−04	−3·4807E−05	−7·4314E−06	7·8271E−05	−2·6942E−05	−1·3048E−05	−4·6649E−05	−7·5829E−06	−2·0372E−07
0·2467	1·0163	−4·0087E−04	−7·8040E−05	−1·5065E−05	2·2054E−04	−6·9905E−05	−2·4112E−05	−1·0026E−04	−1·4405E−05	−8·6771E−07
0·3691	1·0358	−5·8286E−04	−1·3644E−04	−2·3307E−05	4·8324E−04	−1·4130E−04	−3·1919E−05	−1·6604E−04	−2·0265E−05	−2·3774E−06
0·6110	1·0938	−8·7661E−04	−3·1160E−04	−4·4636E−05	1·5289E−03	−3·8961E−04	−3·7574E−05	−3·4128E−04	−3·2012E−05	−9·0669E−06
0·8493	1·1711	−1·0513E−03	−5·5928E−04	−7·8817E−05	3·3876E−03	−7·5844E−04	−3·5174E−05	−5·6381E−04	−5·2309E−05	−2·2353E−05
1·0846	1·2620	−1·1078E−03	−8·5091E−04	−1·3212E−04	6·0455E−03	−1·1826E−03	−2·9317E−05	−8·0606E−04	−8·9080E−05	−4·4501E−05
1·3179	1·3625	−1·0726E−03	−1·1525E−03	−2·0673E−04	9·3905E−03	−1·5906E−03	−1·7053E−05	−1·0415E−03	−1·4375E−04	−7·7402E−05
1·5498	1·4701	−9·7915E−04	−1·4373E−03	−3·0068E−04	1·3281E−02	−1·9283E−03	1·0806E−05	−1·2525E−03	−2·1256E−04	−1·2161E−04
1·7807	1·5832	−8·5658E−04	−1·6888E−03	−4·0922E−04	1·7584E−02	−2·1644E−03	6·5464E−05	−1·4302E−03	−2·8959E−04	−1·7610E−04
2·0109	1·7006	−7·2551E−04	−1·8998E−03	−5·2641E−04	2·2187E−02	−2·2862E−03	1·5668E−04	−1·5721E−03	−3·6899E−04	−2·3859E−04
2·2406	1·8215	−5·9861E−04	−2·0691E−03	−6·4636E−04	2·7001E−02	−2·2948E−03	2·9102E−04	−1·6798E−03	−4·4606E−04	−3·0620E−04
2·4700	1·9455	−4·8262E−04	−2·1995E−03	−7·6400E−04	3·1961E−02	−2·1990E−03	4·7151E−04	−1·7570E−03	−5·1753E−04	−3·7597E−04

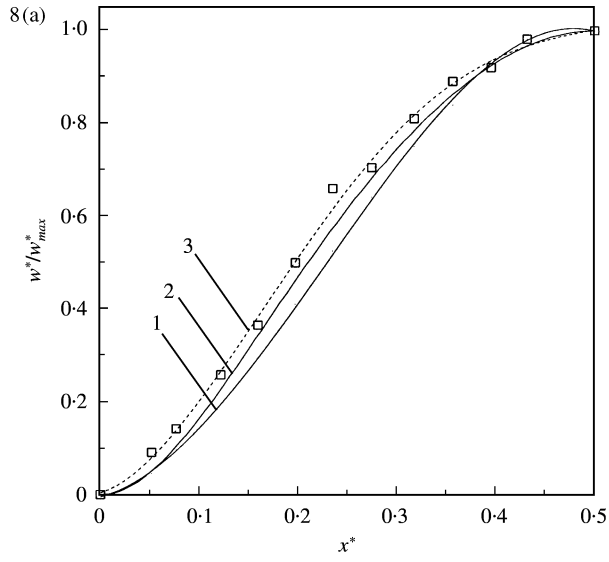

Figure 8(a). Comparison of the normalized first-harmonic component along the length direction for $y^* = 0{\cdot}5$ and $\alpha = 2/3$ CFRP plate $W^*_{max} = 0{\cdot}5$. Curve 1, linear; curve 2, non-linear (th.); curve 3, non-linear (exp.).

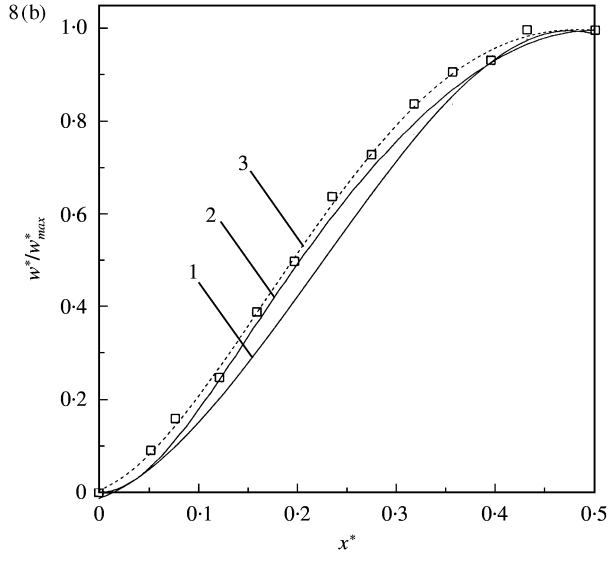

Figure 8(b). Comparison of the normalized first-harmonic component along the length direction for $y^* = 0{\cdot}5$ and $\alpha = 2/3$ CFRP plate $W^*_{max} = 0{\cdot}8$. Curve 1, linear; curve 2, non-linear (th.); curve 3, non-linear (exp.).

the amplitude of vibration which may be reached experimentally. To reach very high amplitudes, an aerodynamic exciter, such as that used in reference [43], has to be used. This exceeded the scope of the limited experimental program performed in this work. However, experimental investigations have an important role to play before and after the theoretical work. Before, because they guide the choice of the basic assumptions and indicate the qualitative trends; after, because they permit validation of the numerical results, to indicate the range of validity and the degree of accuracy of each type of solution. Figure 8(a) and 8(b)

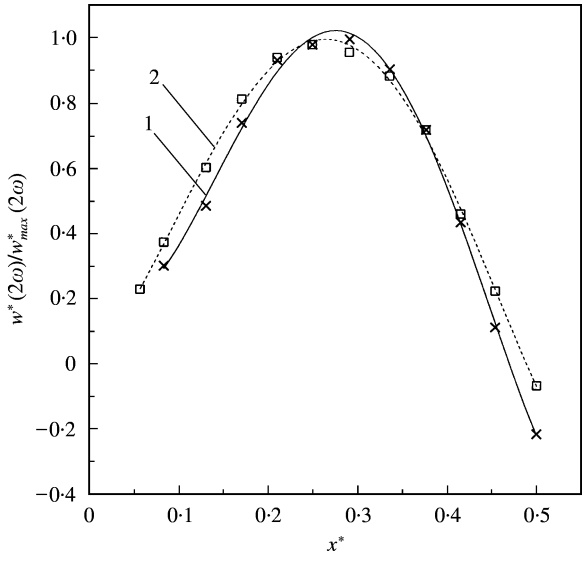

Figure 9. Normalized second-harmonic component along the length direction for $y^* = 0{\cdot}5$. CFRP plate. Curve 1, second harmonic associated with the first harmonic plotted in Figure 4(a) (exp.); curve 2, second harmonic associated with the first harmonic plotted in Figure 4(b) (exp.).

shows the measured normalized separated first-harmonic component along the length direction for maximum non-dimensional amplitudes w^*_{max} of 0·5 and 0·8 together with the normalized theoretical linear and non-linear mode shape. As may be expected, due to the rigidity introduced in the theory by the truncation of the series in the spectral expansion of the displacement function, the theoretical curve is higher than the experimental one. It can be seen that the two curves (non-linear prediction and measured values) are very close to each other. However, although the non-linear experimental and theoretical curves do not coincide exactly, which may be expected due to various experimental errors and theoretical approximations, such as those mentioned above, it can be seen that the trends of deformation of the non-linear mode shapes are very similar. The normalized separate second-harmonic component spatial distribution corresponding to the above two sets of measurements is shown in Figure 9. A shape similar to the plate second mode in the length direction can be observed, confirming the results obtained in the isotropic plate case in references [42, 43]. Also, the normalized second-harmonic spatial distribution appears to be amplitude dependent, with a shift of maximum points towards the clamps. This recalls the amplitude dependence of the second clamped–clamped beam non-linear mode shape obtained theoretically in reference [1].

However, the good agreement between the non-dimensional first non-linear mode shape calculated from the theoretical model and experimental measurements of a fully clamped CFRP plate, indicates once again that this theoretical model based on Hamilton's principle and spectral analysis can be a good tool for analyzing geometrically non-linear free vibration problems.

The numerical results given here, for high amplitudes and low plate aspect ratios, must be considered with some reservation until further investigations determine accurately how other non-linear effects, such as high in-plane displacements, delamination initiation, or change of material behaviour from elastic to plastic may affect the results. Although consideration of such effects exceeded the scope of the present work, it is thought that the

extension of the present theory to include the first effect may be made by using adequate in-plane displacement functions and taking into account their contribution to the total strain energy. Solutions obtained from such a formulation may determine accurately the contribution of the in-plane displacements to the axial stresses and contribute to clarify the question of the domain of validity of the Berger approximation, which has been a subject of much discussion in the literature [38]. Also, higher non-linear modes of fully clamped rectangular laminated plates may be considered, by solving in each case the appropriate set of non-linear algebraic equations.

Figure 10(a–c) shows the normalized fundamental mode shape of CFRP plates with various aspect ratios along the line $x^* = 0{\cdot}025$ for different amplitudes. The mode shapes are normalized in such a manner that the maximum obtained at the plate section centre equals unity. The four lines represent the mode shapes at the amplitudes $a_{11} = 0{\cdot}02$, 0·25, 0·55, 1·05 corresponding, for example for a rectangular CFRP plate when $\alpha = 2/3$, to $w^*_{max} = 0{\cdot}1216, 0{\cdot}5955, 1{\cdot}0556$ and 2·4146 respectively. It was noticed that the deformation of the mode shape for different values of the normalized amplitude of vibration is not symmetric along the section $y^* = 0{\cdot}5$. Also, the non-linear mode shape appears to be amplitude dependent, with a shift of the maximum points towards the left as presented. In Figure 11(a–c), the non-linear mode shape corresponding to $x^* = 0{\cdot}975$ for different aspect ratios, i.e., $\alpha = 2/3$, 1 and 3/2, appears to be amplitude dependent, with a shift of the maximum points this time towards the right as presented. This is due to the influence of the fibre orientation inducing significant contributions of the non-symmetric functions. In Figure 12(a and b), sections of the non-linear mode shape corresponding to $x^* = 0{\cdot}5$ and $y^* = 0{\cdot}5$ cross the corresponding sections of the theoretical linear mode shape at values of (x^*, y^*) corresponding approximately to the quarter dimension of the plate. This characteristic appeared previously in both experimental and theoretical curves given in references [2, 43] for fully clamped isotropic plates. In Part II of this series of papers, the fibre orientation effect will be presented and discussed in more detail.

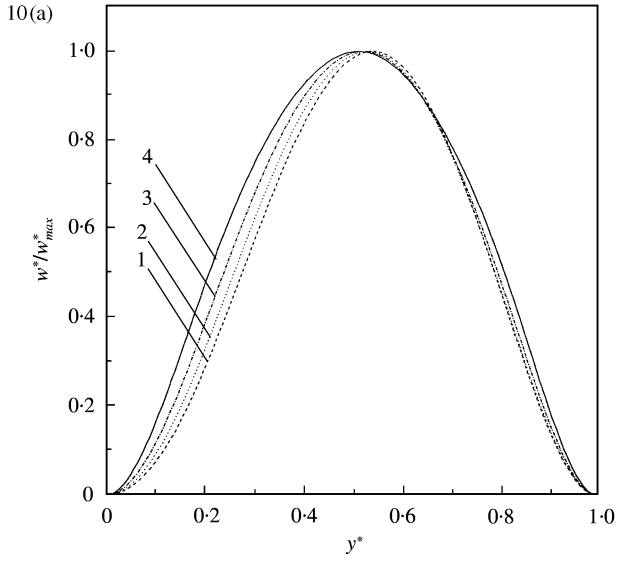

Figure 10(a). Normalized first non-linear mode rectangular CFRP plate $\alpha = 2/3$, $x^* = 0{\cdot}025$. Curve 1, lowest amplitude; curve 4, highest amplitude.

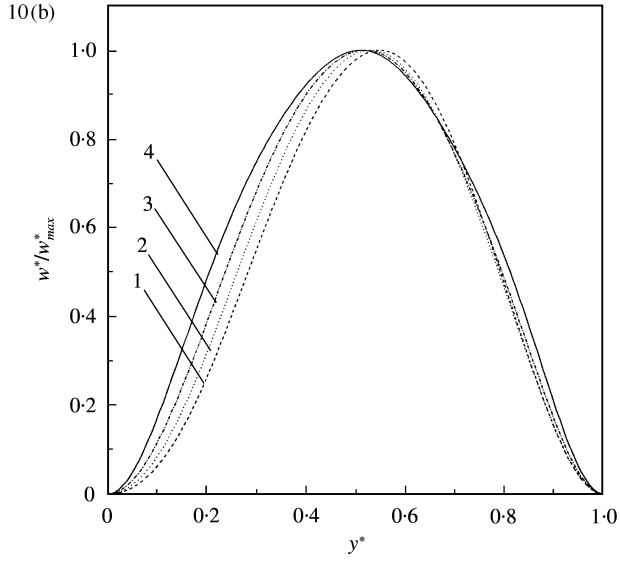

Figure 10(b). Normalized first non-linear mode rectangular CFRP plate $\alpha = 1$, $x^* = 0{\cdot}025$. Curve 1, lowest amplitude; curve 4, highest amplitude.

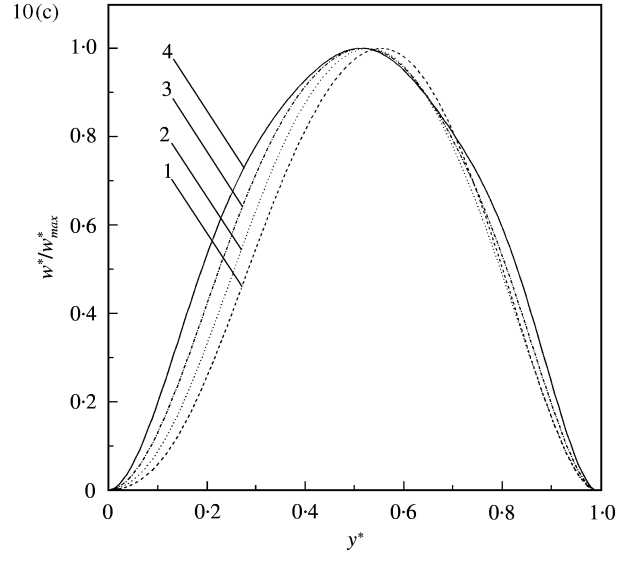

Figure 10(c). Normalized first non-linear mode rectangular CFRP plate $\alpha = 3/2$, $x^* = 0{\cdot}025$. Curve 1, lowest amplitude; curve 4, highest amplitude.

5.4. BENDING STRESSES ASSOCIATED WITH THE FIRST NON-LINEAR MODE SHAPE FOR A FULLY CLAMPED CFRP RECTANGULAR PLATE 2

The non-dimensional bending stress distribution for the CFRP plate considered is plotted in Figures 13–15 for different normalized sections and aspect ratios. As found by Benamar *et al.* [2], it can be seen in Figure 13(a) that the bending stress can exhibit in the

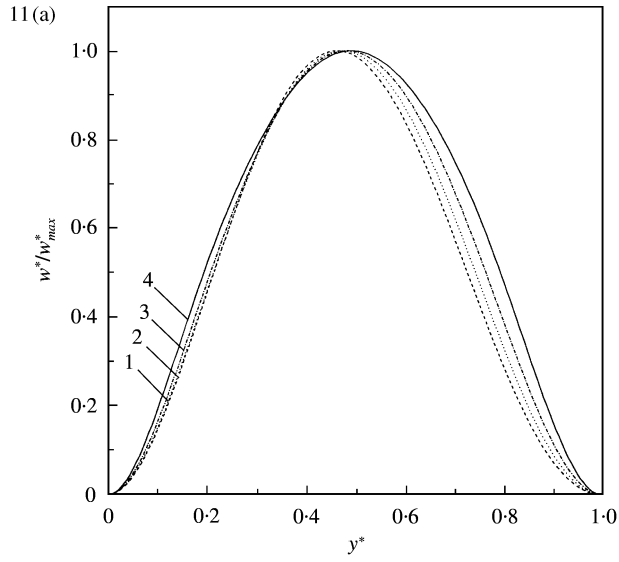

Figure 11(a). Normalized first non-linear mode rectangular CFRP plate $\alpha = 2/3$, $x^* = 0{\cdot}975$. Curve 1, lowest amplitude; curve 4, highest amplitude.

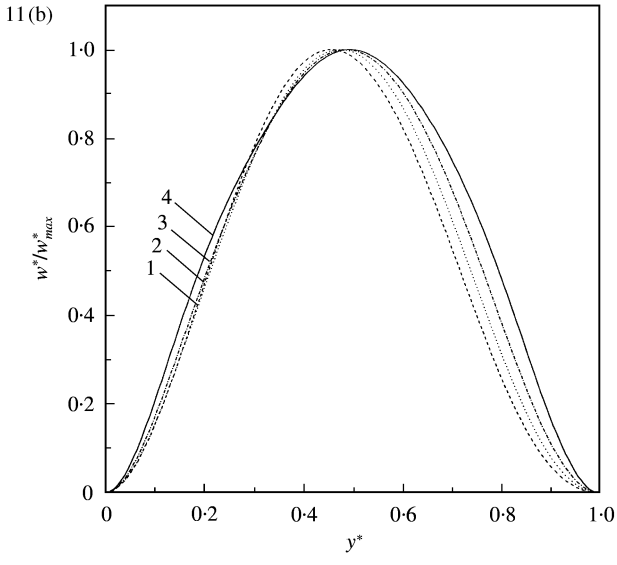

Figure 11(b). Normalized first non-linear mode rectangular CFRP plate $\alpha = 1$, $x^* = 0{\cdot}975$. Curve 1, lowest amplitude; curve 4, highest amplitude.

neighbourhood of the clamps, a distribution with positive bending stresses along the whole section. This is due to the Poisson ratio effect and to high curvatures in the other direction (i.e., the x direction in the present case). In Figures 13–15 a high increase of the bending stress is shown near the clamps. Also, the numerical results show an increase of the non-dimensional non-linear bending stress distribution with increasing a_{11} which is much higher than that obtained for linear vibration of CFRP plates of identical aspect ratio. Although the use of nine plate functions yields a good estimate for the non-linear resonant

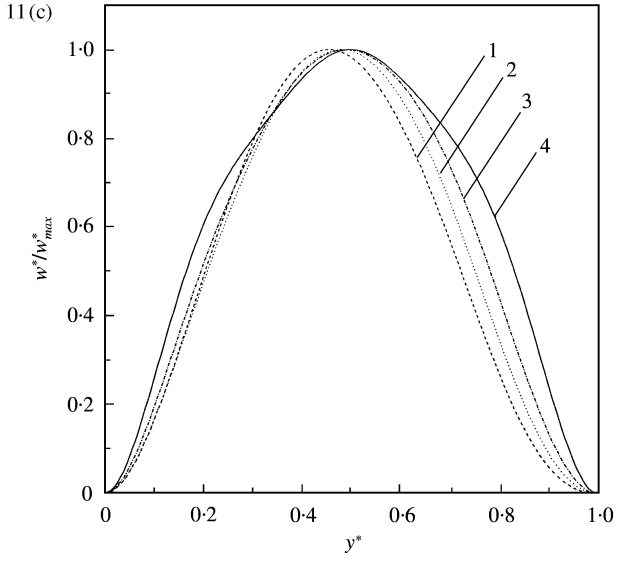

Figure 11(c). Normalized first non-linear mode rectangular CFRP plate $\alpha = 3/2$, $x^* = 0{\cdot}975$. Curve 1, lowest amplitude; curve 4, highest amplitude.

frequency as shown in Figure 16, 18 plate functions should be taken into account in the non-linear bending stress calculations, as can be seen in Figure 17 which shows the difference between the non-dimensional bending stress distribution obtained by using nine plate functions and 18 functions. The quite large difference is due to the nine other contributions taken into account in the present work. In Figure 18, the non-dimensional amplitude dependence of the non-linear bending stress at the point $(x^*, y^*) = (0{\cdot}025, 0{\cdot}025)$

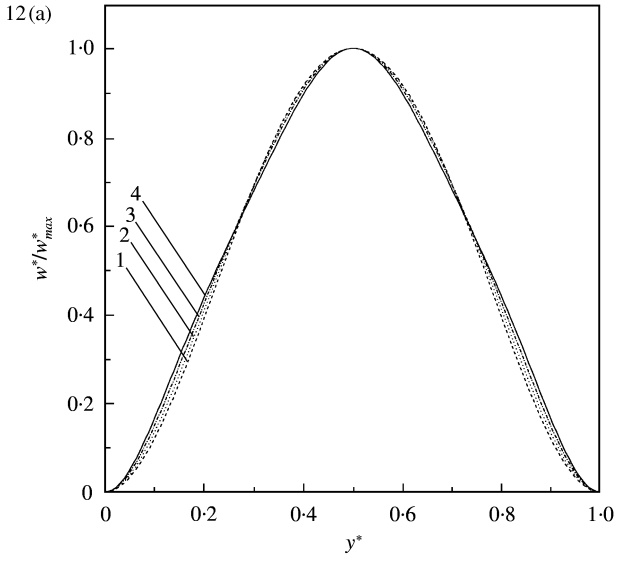

Figure 12(a). Normalized first non-linear mode rectangular CFRP plate $\alpha = 2/3$, $x^* = 0{\cdot}5$. Curve 1, lowest amplitude; curve 4, highest amplitude.

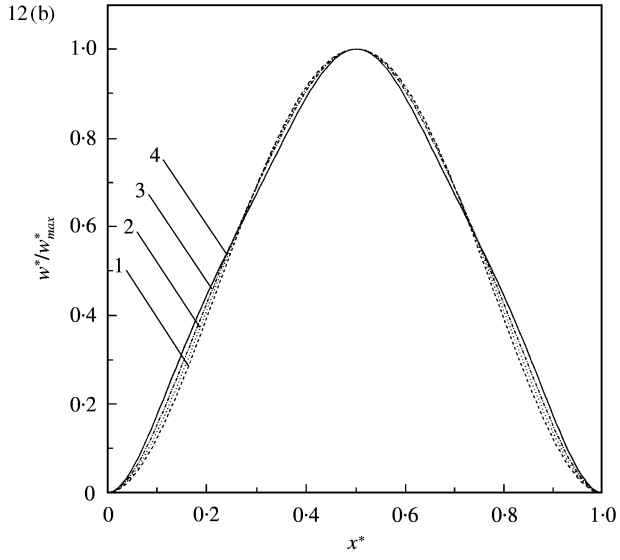

Figure 12(b). Normalized first non-linear mode rectangular CFRP plate $\alpha = 2/3$, $y^* = 0{\cdot}5$. Curve 1, lowest amplitude; curve 4, highest amplitude.

of a fully clamped CFRP rectangular plate having an aspect ratio $\alpha = 2/3$ obtained by using nine and 18 plate functions is compared with that obtained by linear analysis. It can be seen that for $a_{11} = 1{\cdot}05$, which corresponds to $w^*_{max} = 2{\cdot}4146$, the value of non-dimensional linear bending stress is 1·2432 while the corresponding value of the non-dimensional non-linear bending stress obtained by using nine and 18 plate functions are 3·4994 and

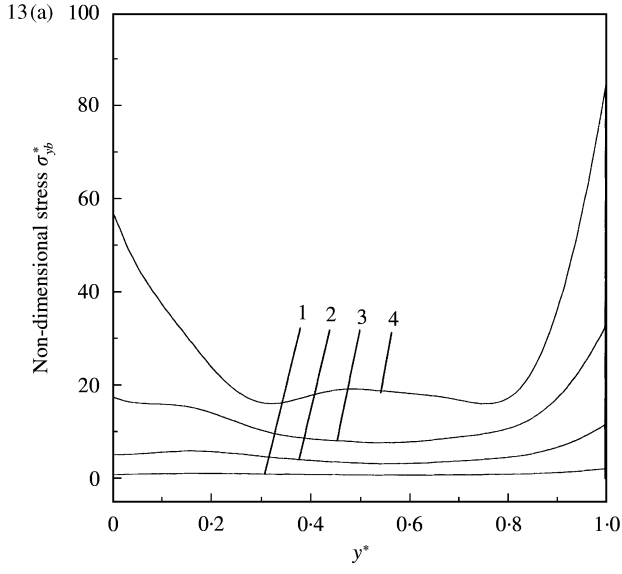

Figure 13(a). Non-dimensional bending stress distribution associated with the fully clamped rectangular CFRP plate 2 first non-linear mode for $\alpha = 2/3$ along the section $x^* = 0{\cdot}025$. Curve 1, lowest amplitude; curve 4, highest amplitude.

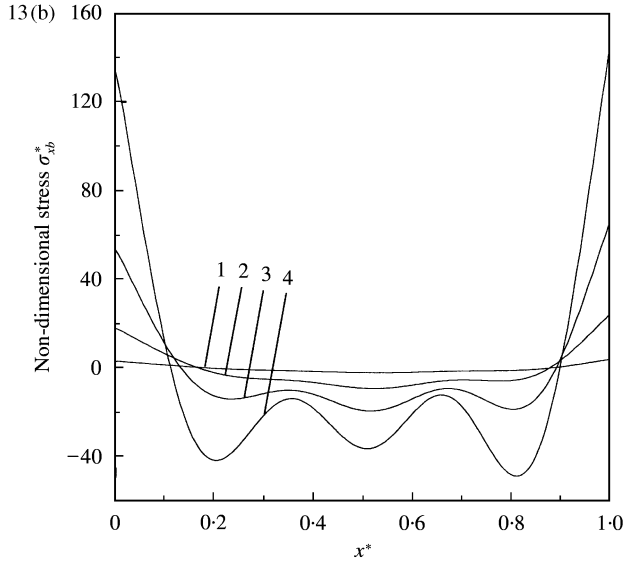

Figure 13(b). Non-dimensional bending stress distribution associated with the fully clamped rectangular CFRP plate 2 first non-linear mode for $\alpha = 2/3$ along the section $y^* = 0{\cdot}25$. Curve 1, lowest amplitude; curve 4, highest amplitude.

3·9789 respectively. This result indicates once again the effect of using 18 plate functions instead of nine especially when calculating the stress distribution. Table 13 summarizes some numerical data concerning the rate of increase in bending stresses. With increasing w^*_{max} the non-dimensional bending stress at the point $A(x^* = 0{\cdot}025, y^* = 0{\cdot}025)$ of the

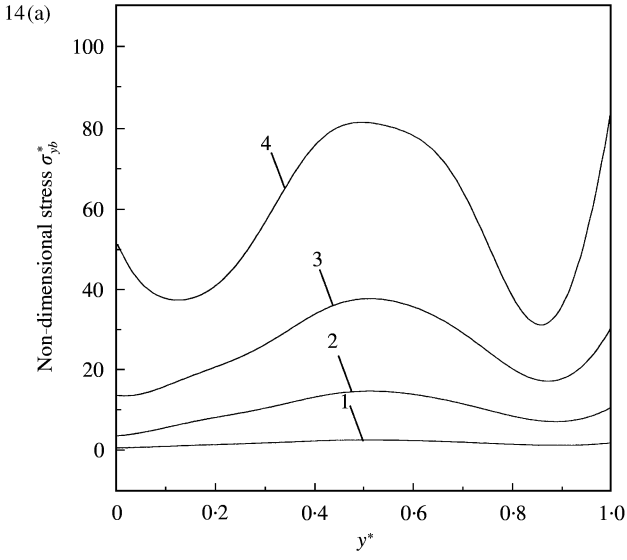

Figure 14(a). Non-dimensional bending stress distribution associated with the fully clamped rectangular CFRP 2 plate first non-linear mode for $\alpha = 1$ along the section $x^* = 0{\cdot}025$. Curve 1, lowest amplitude; curve 4, highest amplitude.

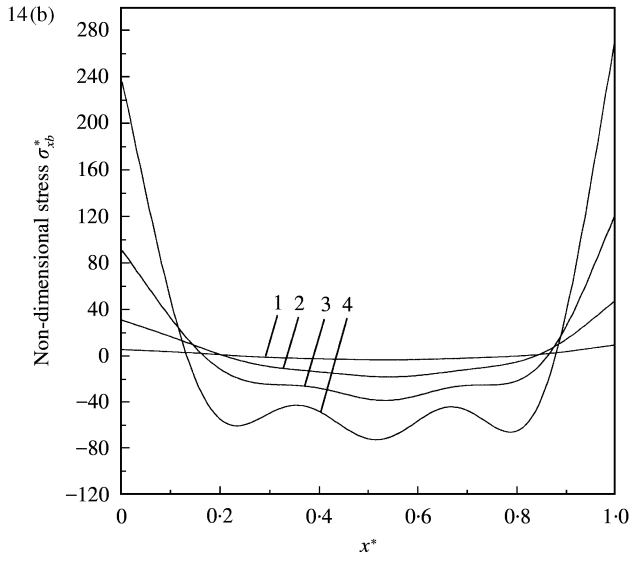

Figure 14(b). Non-dimensional bending stress distribution associated with the fully clamped rectangular CFRP 2 plate first non-linear mode for $\alpha = 1$ along the section $y^* = 0{\cdot}25$. Curve 1, lowest amplitude; curve 4, highest amplitude.

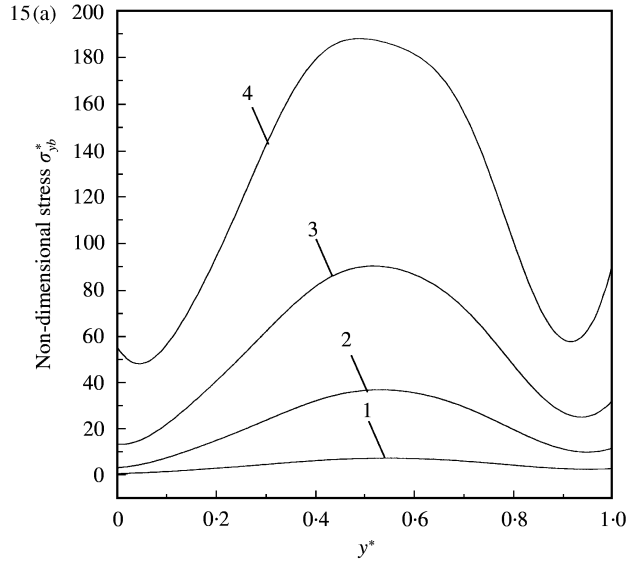

Figure 15(a). Non-dimensional bending stress distribution associated with the fully clamped rectangular CFRP 2 plate first non-linear mode for $\alpha = 3/2$ along the section $x^* = 0{\cdot}025$. Curve 1, lowest amplitude; curve 4, highest amplitude.

CFRP plate examined here corresponding to $\alpha = 2/3$, increases from 0·0598 to 3·9789, when the non-dimensional amplitude increases from 0·1216 to 2·4146, as indicated in Table 13. This is about 3 times the increase expected in the linear theory.

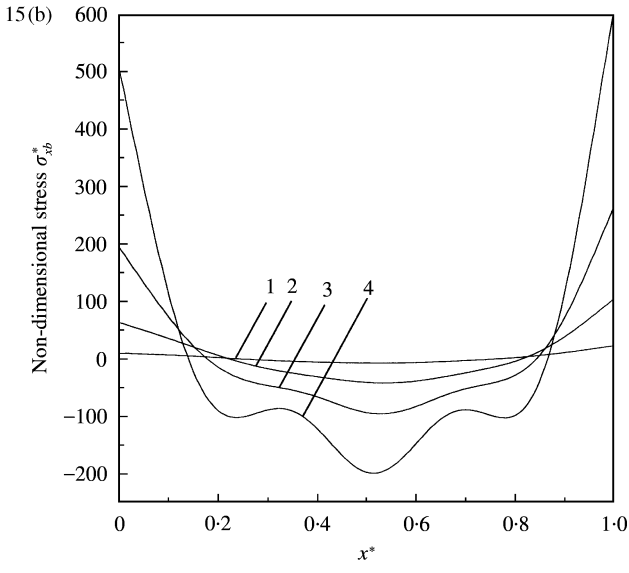

Figure 15(b). Non-dimensional bending stress distribution associated with the fully clamped rectangular CFRP 2 plate first non-linear mode for $\alpha = 3/2$ along the section $y^* = 0{\cdot}25$. Curve 1, lowest amplitude; curve 4, highest amplitude.

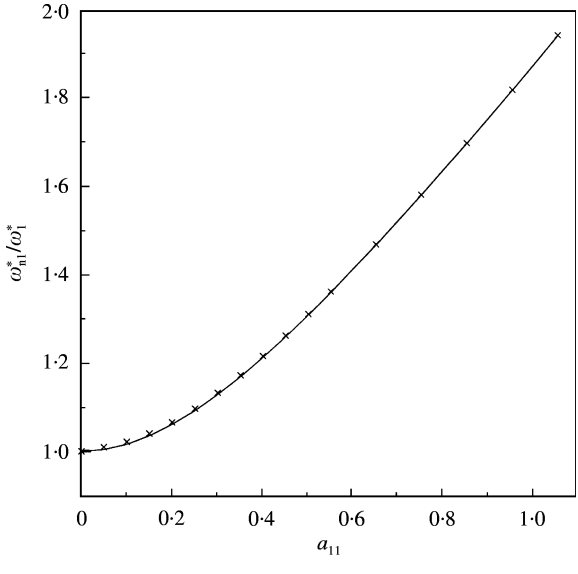

Figure 16. Comparison of the change in natural frequency at large amplitudes for the fully clamped rectangular CFRP plate 2 for $\alpha = 3/2$. ——, 18 plate functions; ×, nine plate functions.

6. CONCLUSIONS

The theoretical model established and applied to beams, plates and shells [1–4], has been successfully applied to calculate the first non-linear mode shape of fully clamped rectangular symmetrically laminated CFRP plates for various aspect ratios. The model was

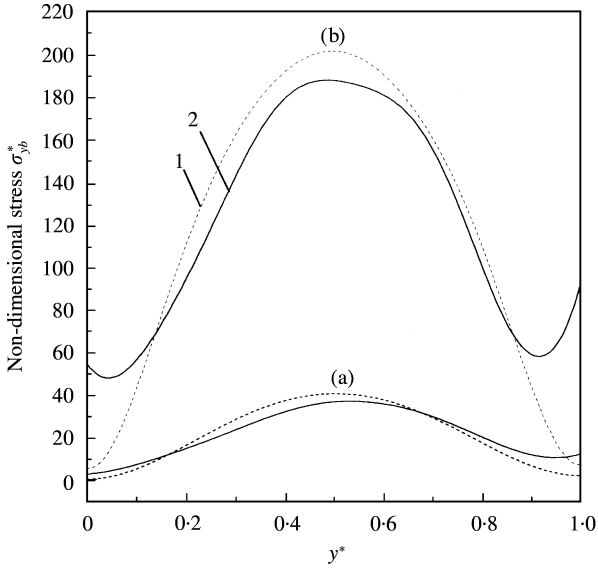

Figure 17. Non-dimensional bending stress distribution associated with the fully clamped rectangular CFRP plate 2 first non-linear mode for $\alpha = 3/2$ along the section $x^* = 0{\cdot}025$. Curve 1, nine plate functions; curve 2, 18 plate functions. (a): $W^*_{max} = 0{\cdot}6110$; (b): $W^*_{max} = 2{\cdot}4700$.

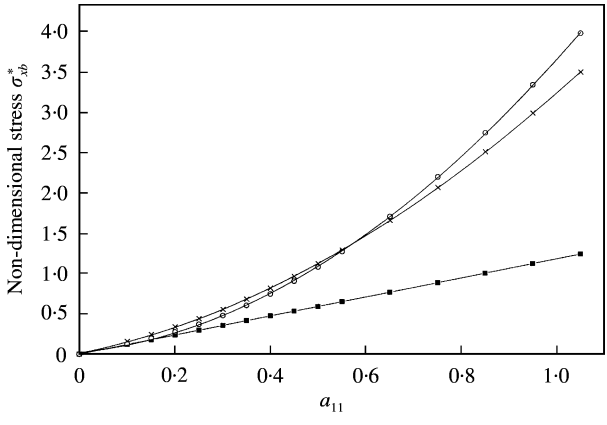

Figure 18. Comparison between the first linear and non-linear non-dimensional bending stress distribution at the point ($x^* = 0{\cdot}025$, $y^* = 0{\cdot}025$) of fully clamped CFRP rectangular plate 2, $\alpha = 2/3$. —■—, linear; ×, nine plate functions; ○, 18 plate functions.

TABLE 13

Comparison of the rate of increase of the non-dimensional bending stress σ^*_{xb} *with increasing* W^*_{max} *at various points* $A(x^*, y^*) = (0{\cdot}025;\ 0{\cdot}025)$; B:$(0{\cdot}25; 0{\cdot}025)$; C:$(0{\cdot}5; 0{\cdot}025)$; D:$(0{\cdot}025; 0{\cdot}25)$; R($W^*$): *rate of increase of* W^*_{max}; R(σ^*_{xb}): *rate of increase of* σ^*_{xb}; *The reference value is the first value*; CFRP *rectangular plate* 2, $\alpha = 2/3$

ω^*_{nl}/ω^*_l	W^*_{max}	R(W^*)	σ^*(A)	R(σ^*(A))	σ^*(B)	R(σ^*(B))	σ^*(C)	R(σ^*(C))	σ^*(D)	R(σ^*(D))
1·002	0·1216		0·0598		1·6684		3·0682		2·6226	
1·1678	1·2818	10·5411	1·2765	21·3462	23·034	13·8060	35·5416	11·5839	42·0694	16·0411
1·5641	2·4146	19·8569	3·9789	66·5367	53·5147	32·0755	75·2650	24·2650	99·2291	37·8362

validated by comparison with experimental results. Excellent agreement has been found between the non-linear frequency of the first mode at small vibration amplitudes from the present model and that obtained by linear analysis.

As has been shown in this work, the fundamental non-linear mode shape of the fully clamped rectangular CFRP symmetrically laminated plate can be obtained with sufficient accuracy by using 18 basic plate functions. This provides a more accurate description of the non-linear mode shape, compared with previous results based on the use of nine symmetric basic plate functions, since it allows the non-symmetry induced by the fibre orientation to be taken into account.

The measurements presented in this work show how the non-linear behaviour of fully clamped CFRP plates at large displacement amplitudes can be complex and different from that expected from linear theory. The measured plate deflection shape at large vibration amplitudes exhibit the same trends of dependence on the amplitude of vibration as those obtained theoretically. This indicates that the theoretical model could be a good tool for analyzing the geometrically non-linear free vibration problems of laminated plates. Experimental investigation of the second harmonic spatial distribution has shown that the second mode can be excited, due to the non-linearity, even if the excitation frequency is close to the resonance frequency of the fundamental mode and the excitation force is applied in a nodal point of the second mode. This result has been established previously in the case of an isotropic plate.

Numerical data corresponding to various values of plate aspect ratio are presented, which may be useful in engineering applications. Comparison of the changes in non-linear resonance frequency at large vibration amplitudes for isotropic and CFRP plates show an increase of the non-dimensional non-linear frequency parameter with increasing a_{11} for the first mode, which is much greater for the CFRP plate than that obtained for an isotropic plate.

The study of the first non-linear mode shape for the CFRP plates considered has shown that the curvature near the edge increases very rapidly with increase of the vibration amplitude. The mode shape near the centre of the plate becomes flatter when the mode amplitude increases. It was also noticed that the deformation of the mode shape, for a given value of the normalized amplitude of vibration, increases as the aspect ratio α increases. The non-dimensional bending stress distribution associated with the CFRP rectangular plate first non-linear mode shows an increase with increasing a_{11} which is much higher than that obtained for a linear vibration for CFRP plates of identical aspect ratio. As a consequence of the deformation of the mode shape, it was shown that the rate of increase in the induced bending stresses in a region close to the clamps can be about 3 times the increase expected in the linear theory. Also, the non-dimensional bending stress distribution associated with the CFRP rectangular plate first non-linear mode for different amplitudes of vibration show a non-symmetry along the length of the section considered; this is due to the influence of the fibre orientation. It is worth noting here that further investigations are needed in order to check the distribution of the non-linear bending stresses obtained at very high amplitudes of vibration.

Further work is needed to investigate the behaviour of higher modes, the effects of fibre orientation, and forced response problems. Investigations are needed to develop a computational method for the analysis of the harmonic distortion spatial distribution induced by large vibration amplitudes of fully clamped CFRP plates. Also, further works are needed to include U and V in the analysis of non-linear vibration in order to calculate the total non-linear stress.

REFERENCES

1. R. BENAMAR, M. M. K. BENNOUNA and R. G. WHITE 1991 *Journal of Sound and Vibration* **149**, 179–195. The effects of large vibration amplitudes on the fundamental mode shape of thin elastic structures. Part I: simply supported and clamped–clamped beams.
2. R. BENAMAR, M. M. K. BENNOUNA and R. G. WHITE 1993 *Journal of Sound and Vibration* **164**, 295–316. The effects of large vibration amplitudes on the fundamental mode shape of thin elastic structures. Part II fully clamped rectangular isotropic plates.
3. R. BENAMAR, M. M. K. BENNOUNA and R. G. WHITE 1990 *Proceedings of the Fourth International Conference on Recent Advances in Structural Dynamics, Southampton.* The effects of large vibration amplitudes on the fundamental mode shape of a fully clamped, symmetrically laminated rectangular plate.
4. F. MOUSSAOUI, R. BENAMAR and R. G. WHITE 2000 *Journal of Sound and Vibration* **232**, 917–943. The effects of large vibration amplitudes on the mode shapes and natural frequencies of thin elastic shells. Part I: coupled transverse-circumferential mode shapes of isotropic circular shells of infinite length.
5. M. EL KADIRI, R. BENAMAR and R. G. WHITE 1999 *Journal of Sound and Vibration* **228**, 333–358. The non-linear free vibration of fully clamped rectangular plates: second non-linear mode for various plate aspect ratios.
6. M. V. LOWSON 1989 *Proceedings of the Royal Aeronautical Society Conference on Aerospace Applications of Advanced Materials.* Future use of advanced materials.
7. D. H. MIDDLETON 1990 *Composite Materials in Aircraft Structures.* Harlow: Longman Scientific & Technical.
8. B. HARRAS, K. C. COLE and T. VU-KHANH 1996 *Journal of Reinforced Plastic Composites* **15**, 174–182. Optimisation of the ultrasonic welding of Peek-carbon composites.
9. B. HARRAS, K. C. COLE and T. VU-KHANH 1997 *Twenty-ninth International SAMPE Technical Conference, Orlando, FL, U.S.A.*, Vol. 29, 475–485. Characterisation of the ultrasonically welded Peek-carbon composites.
10. M. M. SCWARTZ 1992 *Composite Materials Handbook.* New York: McGraw-Hill; second edition.
11. R. G. WHITE 1978 *Composites* **9**, 251–258. A comparison of some statistical properties of the responses of aluminium and CFRP plates to acoustic excitation.
12. H. WOLFE 1995 *Ph.D. Thesis, University of Southampton, U.K.* An experimental investigation of nonlinear behaviour of beams and plates excited to high levels of dynamic response.
13. R. G. WHITE 1988 *Proceedings of the 25th AIAA/ASME Structures, Structural Dynamics and Materials Conference, Williamsburg, U.S.A.*, Paper 88-2242, 253–260. The acoustic excitation and fatigue of composite plates.
14. R. G. WHITE 1990 *Composite Structures* **16**, 171–192. Developments in the acoustic fatigue design process for composite aircraft structures.
15. A. W. LEISSA 1984 *Proceedings of the Second International Conference on Recent Advances in Structural Dynamics, Southampton.* Nonlinear analysis of plate and shell vibrations.
16. M. M. K. BENNOUNA 1981 *Ph.D. Thesis, Institute of Sound and Vibration Research.* Non-linear behaviour of a clamped–clamped beam with consideration of fatigue life.
17. R. BENAMAR 1990 *Ph.D. Thesis, Institute of Sound and Vibration Research.* Non-linear dynamic behaviour of fully clamped beams and rectangular isotropic and laminated plates.
18. A. W. LEISSA 1969 *Vibration of Plates, NASA SP*-160. Washington, DC: US Government Printing Office.
19. A. W. LEISSA 1973 *Journal of Sound and Vibration* **31**, 257–293. The free vibration of rectangular plates.
20. M. SATHYAMOORTHY 1987 *Applied Mechanical Reviews* **40**, 1553–1561. Nonlinear vibration analysis of plates: a review and survey of current developments.
21. K. M. WHITNEY and A. W. LEISSA 1969 *American Society of Mechanical Engineers Journal of Applied Mechanics* **36**, 261–266. Analysis of heterogeneous anisotropic plates.
22. R. G. WHITE 1971 *Journal of Sound and Vibration* **16**, 255–267. Effects of nonlinearity due to large deflections in the resonance testing of structures.
23. R. G. WHITE 1975 *Aero Journal* **79**, 318–325. Some measurements of the dynamic mechanical properties of mixed, carbon fibre reinforced plastic beams and plates.
24. R. G. WHITE and E. M. Y. ABDIN 1985 *Composites* **16**, 293–306. Dynamic properties of aligned short carbon fibre-reinforced plastics in flexure and torsion.

25. R. G. WHITE and R. F. MOUSLEY 1987 *Proceedings of the Fourth International Conference on Composite Structures, Paisley College of Technology*, 1519–1535. Dynamic response of CFRP plates under the action of random acoustic loading.
26. C. F. NG and R. G. WHITE 1988 *Journal of Sound and Vibration* **120**, 1–18. Dynamic behaviour of postbuckled isotropic plates under in-plane compression.
27. C. Y. CHIA 1980 *Nonlinear Analysis of Plates*. New York: Mc-Graw Hill.
28. C. Y. CHIA 1988 *Applied Mechanical Reviews* **41**, 439–451. Geometrically nonlinear behavior of composite plates: a review.
29. L. AZRAR, R. BENAMAR and H. F. WOLFE (to be submitted) *Journal of Sound and Vibration*. Non-linear vibration analysis of beams and plates: a review of the literature and survey of methodological approaches.
30. C. MEI 1973 *Computers and Structures* **3**, 163–174. Finite element displacement method for large amplitude free flexural vibrations of beams and plates.
31. C. MEI and K. DECHA-UMPHAI 1985 *Journal of Sound and Vibration* **102**, 369–380. A finite element method for non-linear forced vibration of beams.
32. C. MEI and K. DECH-UMPHAI 1985 *American Institute of Aeronautics and Astronautics Journal* **23**, 1104–1110. Finite element method for nonlinear forced vibration of rectangular plates.
33. G. VENKATESWARA RAO, K. KANAKA RAJU and I. S. RAJU 1976 *Computers and Structures* **6**, 169–172. Finite element formulation for large amplitude free vibration of beams and orthotropic circular plates.
34. B. S. SARMA and T. K. VARADAN 1983 *Journal of Sound and Vibration* **86**, 61–70. Lagrange-type formulation for finite element analysis of nonlinear beam vibration.
35. W. HAN and M. PETYT 1996 *Computers and Structures* **61**, 705–712. Linear vibration analysis of laminated rectangular plates using the hierarchical finite element method—I: free vibration analysis.
36. W. HAN and M. PETYT 1996 *Computers and Structures* **61**, 713–724. Linear vibration analysis of laminated rectangular plates using the hierarchical finite element method—II: forced vibration analysis.
37. W. HAN and M. PETYT 1997 *Computers and Structures* **63**, 295–308. Geometrically nonlinear vibration analysis of thin, rectangular plates using the hierarchical finite element method—I: the fundamental mode of isotropic plates.
38. W. HAN and M. PETYT 1997 *Computers and Structures* **63**, 309–318. Geometrically nonlinear vibration analysis of thin, rectangular plates using the hierarchical finite element method—II: 1st mode of laminated plates and higher modes of isotropic and laminated plates.
39. P. RIBEIRO and M. PETYT 1999 *International Journal of Mechanical Sciences* **41**, 437–459. Nonlinear vibration of plates by the hierarchical finite element and continuation methods.
40. P. RIBEIRO and M. PETYT 1999 *Journal of Sound and Vibration* **225**, 127–152. Multi-modal geometrical non-linear free vibration of fully clamped composite laminated plates.
41. L. AZRAR, R. BENAMAR and M. POITIER-FERRY 1999 *Journal of Sound and Vibration* **220**, 695–727. An asymptotic-numerical method for large-amplitude free vibrations of thin elastic plates.
42. R. BENAMAR, M. M. K. BENNOUNA and R. G. WHITE 1990 *Proceedings of the Eighth International Modal Analysis Conference, Kissimmee, FL* Vol. 2, 1352–1358. Spatial distribution of the harmonic distortion induced by large vibration amplitudes of fully clamped beams and rectangular plates.
43. R. BENAMAR, M. M. K. BENNOUNA and R. G. WHITE 1994 *Journal of Sound and Vibration* **175**, 377–424. The effects of large vibration amplitudes on the mode shapes and natural frequencies of thin elastic structures. Part III: fully clamped rectangular isotropic plates-measurements of the mode shape amplitude dependence and the spatial distribution of harmonic distortion.
44. L. AZRAR, R. BENAMAR and R. G. WHITE 1999 *Journal of Sound and Vibration* **224** 183–207. A semi-analytical approach to the non-linear dynamic response problem S–S and C–C beams at large vibration amplitudes. Part I: general theory and application to the single mode approach to free and forced vibration analysis.
45. Z. BEIDOURI, R. BENAMAR and R. G. WHITE (to be submitted) *Journal of Sound and Vibration*. The effects of large vibration amplitudes on the mode shapes and natural frequencies of C–C–C–SS rectangular isotropic plates.
46. M. HATERBOUCH, R. BENAMAR and R. G. WHITE (to be submitted) *Journal of Sound and Vibration*. The effects of large vibration amplitudes on the mode shapes and natural frequencies of clamped circular isotropic plates.

47. M. M. K. BENNOUNA and R. G. WHITE 1984 *Journal of Sound and Vibration* **96**, 309–331. The effects of large vibration amplitudes on the fundamental mode shape of a clamped–clamped uniform beam.
48. R. RIBEIRO 1998 *Ph.D. Thesis, University of Southampton*. Geometrical nonlinear vibration of beams and plates by the hierarchical finite element method.
49. W. HAN 1993 *Ph.D. Thesis, Institute of Sound and Vibration Research*. The analysis of isotropic and laminated rectangular plates including geometrical non-linearity using the p-version finite element method.
50. J. E. ASHTON and J. M. WHITNEY 1970 *Theory of Laminated Plates*. Technomic Publication, Stanford, Conn. USA.
51. S. TIMOSHENKO 1959 *Theory of plates and Shells*, 416. New York: McGraw-Hill.
52. S. TIMOSHENKO, S. WEINSOWSKY-KRIEGER and R. M. JONES 1975 *Mechanics of Composite Materials*, 51. International Student Edition, McGraw-Hill Kogakusha, Ltd. Tokyo.
53. P. K. MALLICK 1993 *Fibre-reinforced composites: Materials, Manufacturing and Design*, 152. New York: Marcel Dekker, Inc.; second edition revised and expanded.
54. M. K. PRABHAKARA and C. Y. CHIA 1977 *Journal of Sound and Vibration* **52**, 511–518. Nonlinear flexural vibrations of orthotropic rectangular plates.
55. S. W. TSAI and H. T. HAHN 1980 *Introduction to Composite Materials*, 145. Technomic Publishing Company, Inc., chapter IV. Lancaster, Pensylvania, USA.
56. *Engineering Science Data Unit* (*ESDU*) 1983 Estimation of the stiffnesses and apparent elastic properties of laminated flat plates. Item number 83035.
57. G. C. WRIGHT 1971 *Institute of Sound Vibration Research Technical Report No.* 51. The dynamic properties of fibre reinforced plastic beams.
58. S. ABRATE and G. SCHOEPPNER 1997 *Twenty-ninth International SAMPE* (*Society for the Advancement of Materials and Process Engineering*) *Technical Conference, Orlando, FL*, October 28–November 1, 725–732. Identification of support conditions for composite beams and plates from natural frequencies.
59. A. W. LEISSA 1973 *Journal of Sound and Vibration* **31**, 257–393. Free vibration of rectangular plates.
60. M. J. D. POWELL 1965 *Computer Journal*. **7**, 303–307. A method for minimising a sum of squares of nonlinear functions without calculating derivatives.
61. D. YOUNG 1950 *Journal of Applied Mechanics* **47**, 448–453. Vibration of rectangular plates by the Ritz method.

APPENDIX A: NUMERICAL DETAILS OF THE FULLY CLAMPED SYMMETRICALLY LAMINATED RECTANGULAR PLATE ANALYSIS

A.1. PLATE FUNCTIONS USED

The chosen basic functions $f_i^{a^*}$ were the linear clamped–clamped beam functions [17],

$$f_i^{a^*}(x) = \frac{\mathrm{ch}\,(v_i\,x/L) - \cos(v_i\,x/L)}{\mathrm{ch}\,v_i - \cos v_i} - \frac{\mathrm{sh}\,(v_i\,x/L) - \sin(v_i\,x/L)}{\mathrm{sh}\,v_i - \sin v_i},$$

where v_i for $i = 1, 2, \ldots$ are the eigenvalue parameters for a clamped–clamped beam. The values of the parameters v_i were computed by solving numerically the transcendental equation $\cosh v_i \cos v_i = 1$ and are given in Table A1.

The fully clamped rectangular plate functions w_i^* were defined as

$$w_i^*(x^*, y^*) = \frac{1}{G} f_{\alpha i}^{a^*}(x^*) f_{\beta i}^{a^*}(y^*),$$

in which $x^* = x/L$, $y^* = y/L$, $w_i^*(x^*, y^*) = w_i/H(x/L, y/L)$ and G is a normalization scaling factor given by

$$G = \sqrt{\int_{S^*} (f_{\alpha i}^{a^*}(x^*) f_{\beta i}^{a^*}(y^*))^2 \,\mathrm{d}x^* \,\mathrm{d}y^*},$$

TABLE A1

Symmetric (a) and antisymmetric (b) eigenvalue parameters for a clamped–clamped beam

	(a)		(b)
1	4·73004075	2	7·85320462
3	10·99560784	4	14·13716549
5	17·27875966	6	20·42035225
7	23·56194490	8	26·70353756
9	29·84513021	10	32·98672286
11	36·12831552	12	39·26990817

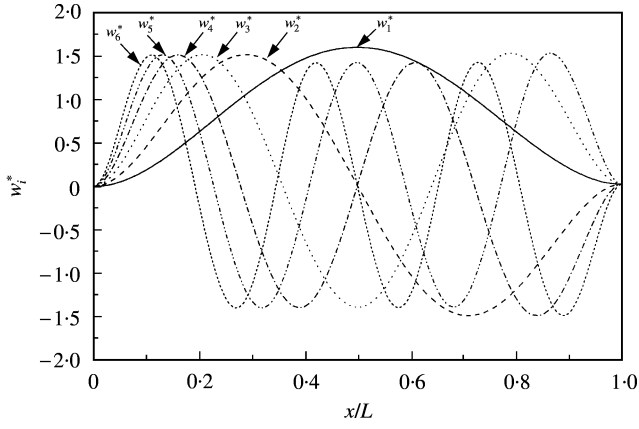

Figure A1. Clamped–clamped beam functions for $i = 1, 2, 3, 4, 5, 6$.

The functions w_i were normalized in such a manner that

$$m_{ij}^* = \int_0^1 w_i^*(x^*) w_j^*(x^*)\,\mathrm{d}x^* = \delta_{ij}.$$

The functions $w_i^* = i, \ldots, 6$, are shown in Figure A1.

A.2. DETAILS OF THE APPLICATION OF HAMILTON'S PRINCIPLE

The dynamic behaviour of the structure is governed by Hamilton's principle, which is symbolically written as

$$\partial \int_0^{2\pi/\omega} (V - T) = 0, \tag{A.1}$$

in which ∂ indicates the variation of the integral. Introducing assumed series (14) into energy condition (A.1) via equations (15) reduces the problem to that of finding the minimum of the

function ϕ given by

$$\phi = \int_0^{2\pi/\omega} (\tfrac{1}{2} a_i a_j k^*_{ij} \sin^2 \omega t + \tfrac{1}{2} a_i a_j a_k a_l b^*_{ijkl} \sin^4 \omega t - \tfrac{1}{2} \omega^2 a_i a_j m^*_{ij} \cos^2 \omega t)\, \mathrm{d}t \tag{A.2}$$

with respect to the undetermined constant a_i. Integration the trigonometric functions $\sin^2 \omega t$, $\sin^4 \omega t$ and $\cos^2 \omega t$ over the range $[0, 2\pi/\omega]$ leads to the following expression:

$$\phi = \frac{\pi}{2\omega} \left(a_i a_j k^*_{ij} + \frac{3}{4} a_i a_j a_k a_l b^*_{ijkl} - \omega^2 a_i a_j m^*_{ij} \right), \tag{A.3}$$

In this expression, ϕ appears as a function of only the undetermined constant, a_i, $i = 1, \ldots, n$. Equation (A.1) reduces to

$$\partial\phi/\partial a_r = 0, \quad r = 1, \ldots, n, \tag{A.4}$$

which can be written as

$$\frac{2\pi}{\omega} \left(\frac{\partial a_i}{\partial a_r} a_j k^*_{ij} + a_i \frac{\partial a_j}{\partial a_r} k^*_{ij} + \frac{3}{4} \frac{\partial a_i}{\partial a_r} a_j a_k a_l b^*_{ijkl} + \frac{3}{4} a_i \frac{\partial a_j}{\partial a_r} a_k a_l b^*_{ijkl} + \frac{3}{4} a_i a_j \frac{\partial a_k}{\partial a_r} a_l b^*_{ijkl} \right.$$

$$\left. + \frac{3}{4} a_i a_j a_k \frac{\partial a_l}{\partial a_r} b^*_{ijkl} - \omega^2 \left(\frac{\partial a_i}{\partial a_r} a_j m^*_{ij} + a_i \frac{\partial a_j}{\partial a_r} m^*_{ij} \right) \right) = 0, \quad r = 1, \ldots, n. \tag{A.5}$$

As

$$\frac{\partial a_i}{\partial a_r} = \delta_{ir}, \quad \frac{\partial a_j}{\partial a_r} = \delta_{jr}, \quad \frac{\partial a_k}{\partial a_r} = \delta_{kr}, \quad \frac{\partial a_l}{\partial a_r} = \delta_{lr}, \tag{A.6}$$

where δ is the Kronecker symbol defined by $\delta_{ij} = 1$ if $i = j$ and $\delta_{ij} = 0$ if $i \neq j$, equations (A.5) lead to

$$(a_j k^*_{ij} + a_i k^*_{ij}) + \tfrac{3}{4}(a_j a_k a_l b^*_{ijkl} + a_i a_k a_l b^*_{ijkl} + a_i a_j a_l b^*_{ijkl} + a_i a_j a_k b^*_{ijkl})$$

$$- \omega^2 (a_j m^*_{ij} + a_i m^*_{ij}) = 0 \quad r = 1, \ldots, n, \tag{A.7}$$

Generally, and this is the case for all the applications of this theory given in reference [14], and presented in this present work, the tensors k^*_{ij} and m^*_{ij} are symmetric, and the tensor b^*_{ijkl} is such that

$$b^*_{ijkl} = b^*_{klij} \quad \text{and} \quad b^*_{ijkl} = b^*_{jikl}. \tag{A.8}$$

Upon taking into account these properties of symmetry, it appears that equations (A.7) are equivalent to the following set of non-linear algebraic equations:

$$2a_i k^*_{ir} + 3a_i a_j a_k b^*_{ijkr} - 2\omega^2 a_i m^*_{ir} = 0, \quad r = 1, \ldots, n. \tag{A.9}$$

A.3. SYMMETRIZATION PROCEDURE FOR THE BENDING AND NON-LINEAR RIGIDITY TENSORS k_{ij}^* *AND* b_{ijkl}^*

Illustration of the symmetrization procedure

Consider the bending strain energy expression (10). The discretization of terms proportional to D_{11}, D_{22} and D_{66} leads to symmetric expressions, with respect to i and j; but the discretization of the other terms leads to expressions which need to be symmetrized in order to obtain a symmetric rigidity matrix k_{ij}^*. For example, the discretization of the term:

$$2D_{12}\frac{\partial^2 W}{\partial y^2}\frac{\partial^2 W}{\partial x^2} \tag{A.10}$$

leads to

$$2D_{12}a_i a_j\frac{\partial^2 w_i}{\partial y^2}\frac{\partial^2 w_j}{\partial x^2}. \tag{A.11}$$

If only two different given values are assigned to the indices i and j, the expression obtained is not symmetric. But, expression (A.11) involves a summation over the repeated indices i and j. So, it may also be written as

$$2D_{12}a_i a_j \times \frac{1}{2}\left[\frac{\partial^2 w_i^*}{\partial y^{*^2}}\frac{\partial^2 w_j^*}{\partial x^{*^2}} + \frac{\partial^2 w_i^*}{\partial x^{*^2}}\frac{\partial^2 w_j^*}{\partial y^{*^2}}\right]. \tag{A.12}$$

This is the form adopted in equation (20) for this term.

A similar procedure has been adopted for the other terms, in order to obtain a symmetric rigidity tensor. Also, a similar procedure has been applied when discretizing the non-linear axial strain energy V_a, in order to fulfil the symmetry requirements $b_{ijkl}^* = b_{klij}^*$ and $b_{ijkl}^* = b_{jikl}^*$.

APPENDIX B: NOMENCLATURE

$\{\varepsilon\}$	column matrix of total strains
$\{\varepsilon^0\}$	column matrix of strains due to the in-plane displacements u, v, w
x, y, z	point co-ordinates
$\{\kappa\}$	column matrix of bending or twisting
$\{\lambda^0\}$	column matrix of strains induced by large displacements W
$\varepsilon_x, \varepsilon_y, \gamma_{xy}$	tensor strain components
$\sigma_x^{(k)}, \sigma_y^{(k)}, \sigma_{xy}^{(k)}$	stresses in the kth layer
$[\bar{Q}]$	6×6 matrix of transformed stiffness
$[\bar{Q}]_k$	6×6 matrix of transformed stiffness for the kth layer
$N_x^{(k)}, N_y^{(k)}, N_{x,y}^{(k)}$	force resultant for the kth layer
$M_x^{(k)}, M_y^{(k)}, M_{x,y}^{(k)}$	moment resultant for the kth layer
h_k	distance from the mid-plane to the layer surface of the kth layer
A_{ij}, B_{ij}, D_{ij}	extensional, coupling and bending stiffness coefficients for the laminated plate
A_{ij}^*, D_{ij}^*	non-dimensional extensional and bending stiffness coefficients
$\{A_k\}^{\mathrm{T}}$	matrix of coefficients corresponding to the kth harmonic
$\{W\}^{\mathrm{T}}$	basic spatial functions matrix
a_{ij}	contribution coefficient of the plate deflection function as a product of the ith and jth beam mode shapes in the x and y directions respectively
a, b	length, width of the plate
E	Young's modulus

H	plate thickness
k_{ij}, m_{ij} and b_{ijkl}	general term of the rigidity tensor, the mass tensor and the non-linearity tensor respectively
k^*_{ij}, m^*_{ij} and b^*_{ijkl}	general term of the non-dimensional rigidity tensor, mass tensor and non-linearity tensor respectively
S, S^*	dimensional and non-dimensional surfaces $[0, a] \times [0, b]$ and $[0, 1] \times [0, 1]$ respectively
$U(x, y, t)$, $V(x, y, t)$	in-plane displacements at point (x, y) of the plate $U(x, y, t) = u(x, y) \sin^2 \omega t$ $V(x, y, t) = v(x, y) \sin^2 \omega t$
V_b, V_a and V	bending, axial and total strain energy respectively
T	kinetic energy
$W(x, y, t)$	transverse displacement at point x on the plate, $W(x, y, t) = w(x, y) \sin \omega t$
$W^*(x, y, t)$	non-dimensional transverse displacement at point x on the plate
w^*_{max}	maximum of the non-dimensional transverse displacement
W_m	represents the maximum amplitude of vibration displacement attained during the cycle at the points (x^*, y^*)
A_m	mode amplitude at the centre of the plate for the fundamental mode
A_m/H	amplitude ratio
W_1	represents the first harmonic at the point (x^*, y^*)
(x^*, y^*)	non-dimensional co-ordinates $(x^* = x/a)$ and $(y^* = y/b)$
α	non-dimensional parameter (aspect ratio) given by $\alpha = a/b$
v_{xy}	major Poisson's ratio
E_x	longitudinal modulus
E_y	transverse modulus
G_{xy}	shear modulus
ρ	mass density per unit volume of the plate
ω, ω^*	frequency and non-dimensional frequency parameter respectively
ω_l, ω_{nl}	linear frequency and non-linear frequency respectively
σ_{xb}, σ_{yb}	dimensional bending stresses
σ^*_{xb}, σ^*_{yb}	non-dimensional dimensional bending stresses